Ab initio computations of deformed nuclei

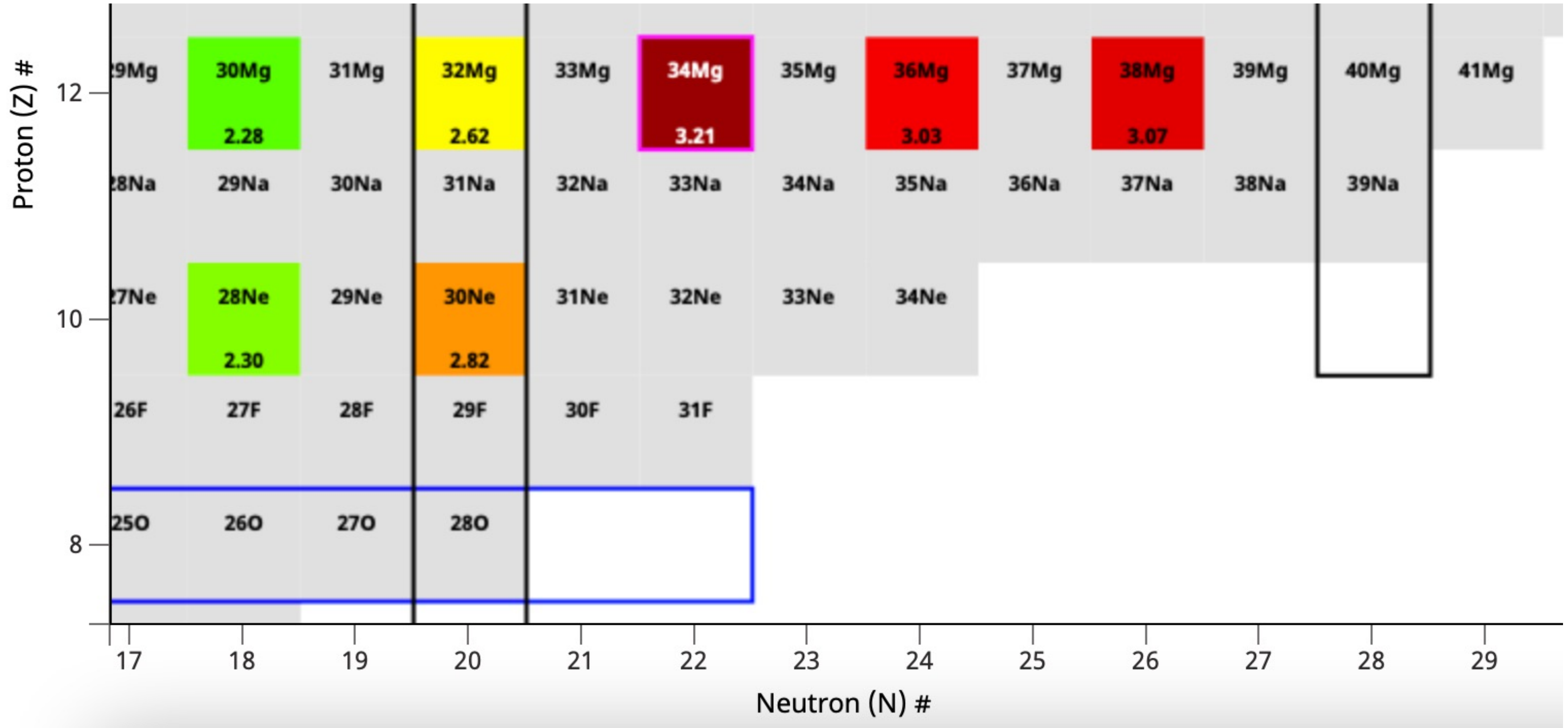

Credit: NNDC

Thomas Papenbrock

University of Tennessee & Oak Ridge National Laboratory

Intersection of nuclear structure and high-energy nuclear collisions

INT, Seattle, 2/15/2023

Work supported by the US Department of Energy

SciDAC Scientific Discovery through Advanced Computing

NUCLEI Nuclear Computational Low-Energy Initiative

Collaborators

- ORNL: G. Hagen, G. Jansen, J. Lietz, **Baishan Hu, Zhonghao Sun**
- U of Tennessee: **Charles Bell**
- Gothenburg: **Weiguang Jiang**, A. Ekström, C. Forssén
- LANL: **Sam Novario**
- Saclay: T. Duguet
- TRIUMF: **Peter Gysbers**, J. D. Holt, P. Navrátil
- TU Darmstadt: **Alex Tichai**

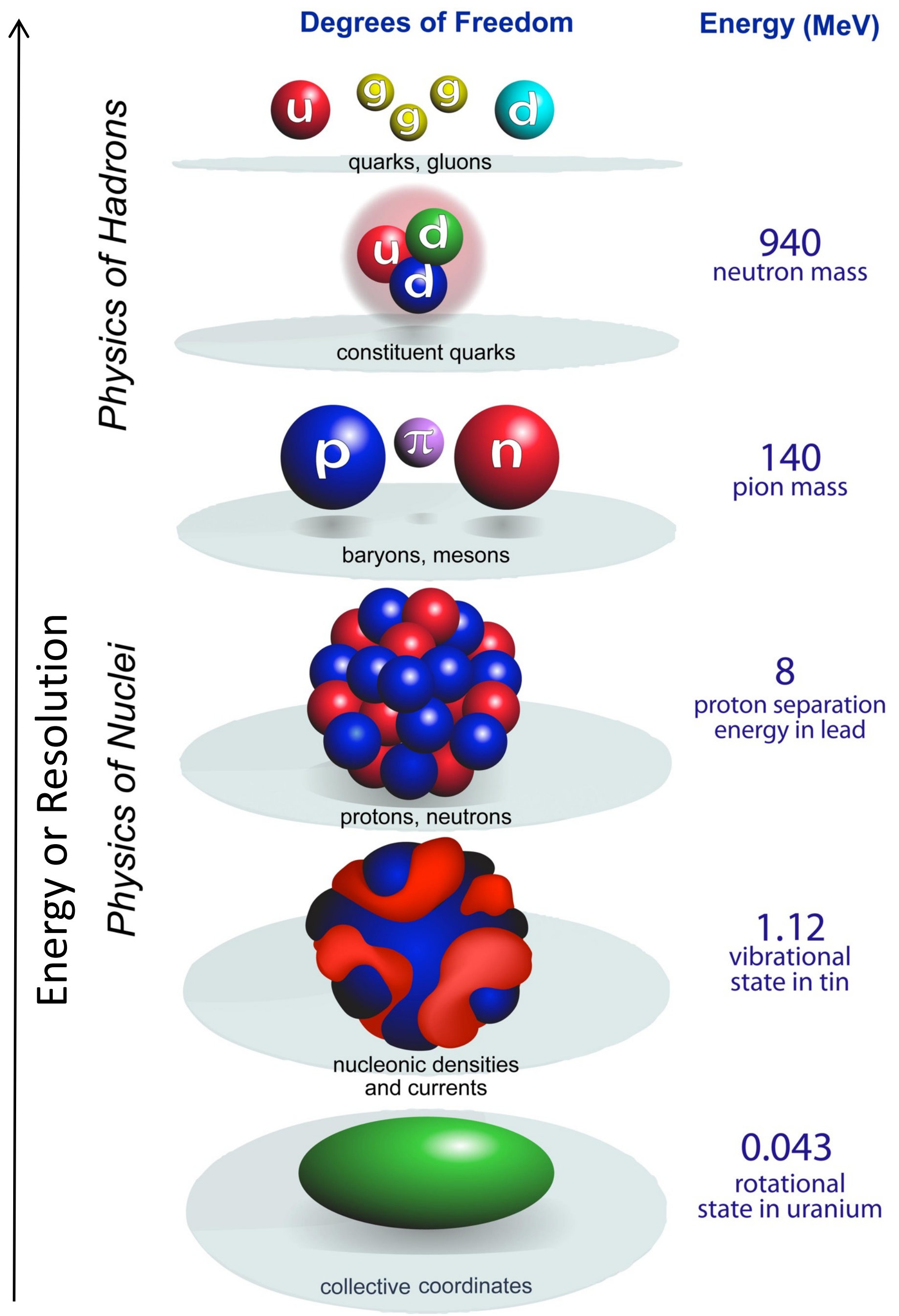

Fig.: Bertsch, Dean, Nazarewicz (2007)

RHIC

Common interests: Simplicity emerging from complex systems?

Low-energy nuclear theory

Aims of this presentation

- Engage with RHIC physicists
- Inform what calculations we can perform
- See where this could lead us

Progress in computing nuclei from EFT Hamiltonians

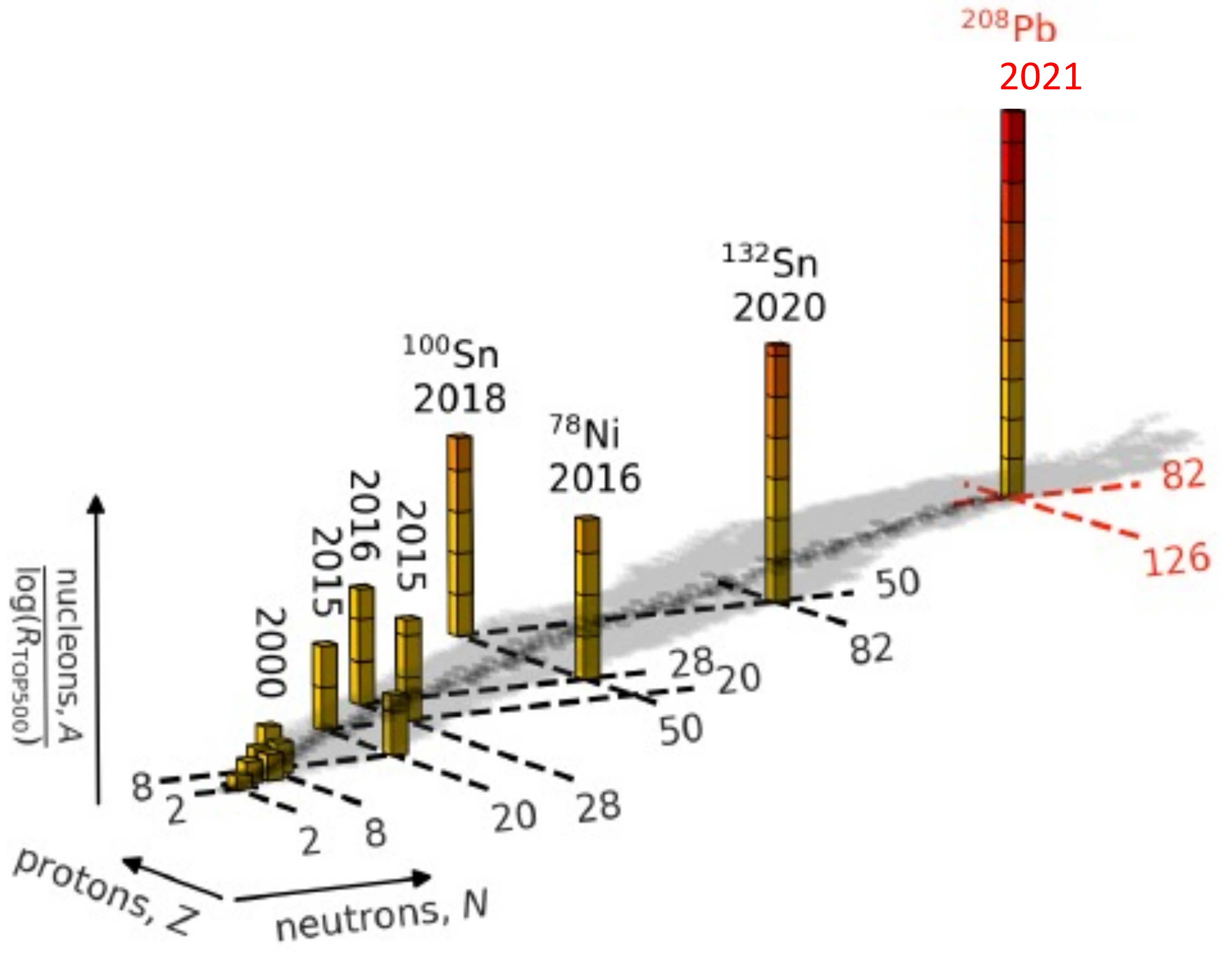

Tremendous progress

- Ideas from EFT and RG
- Methods that scale polynomially with mass number
- Ever-increasing computing powers

1. Ab initio methods not limited to light nuclei
2. Computing nuclei only exponentially hard if one chooses so

1975 Nobel Prize in Physics: Aage Bohr, Ben Mottelson, Leo Rainwater


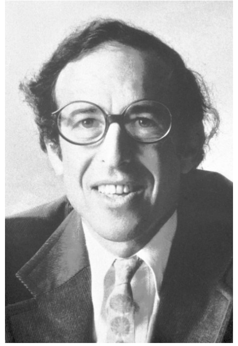


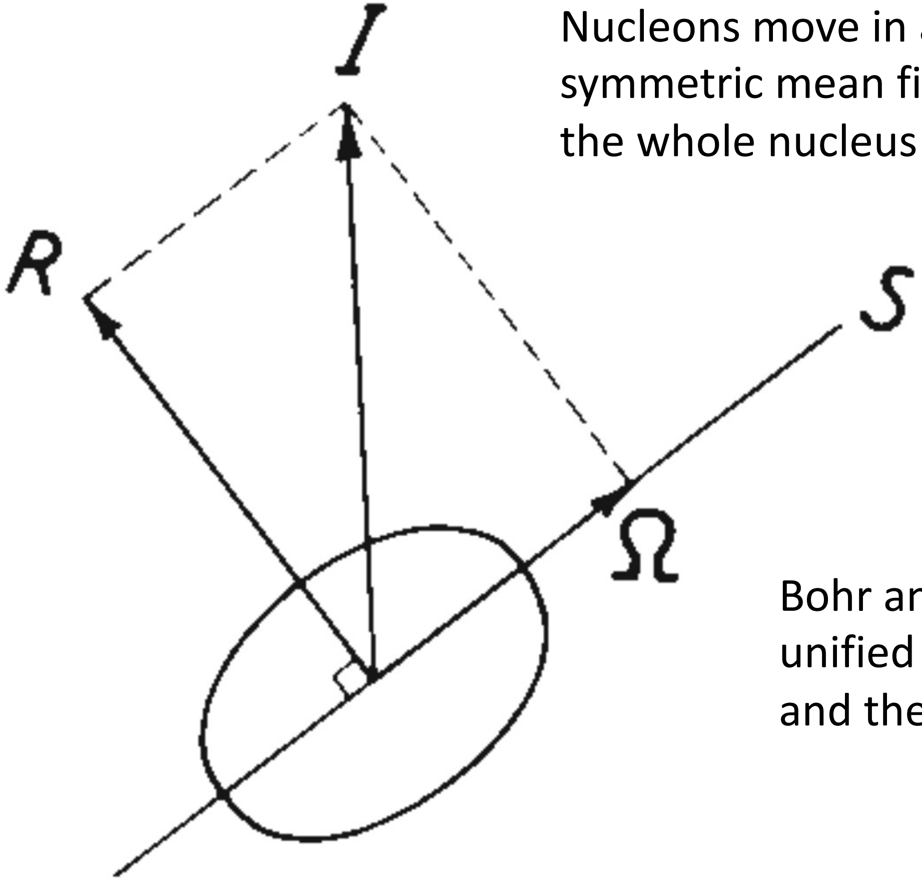

A. Bohr (1950s)

Nucleons move in an axially symmetric mean field and the whole nucleus rotates

Bohr and Mottelson's model unified the spherical shell model and the liquid drop model

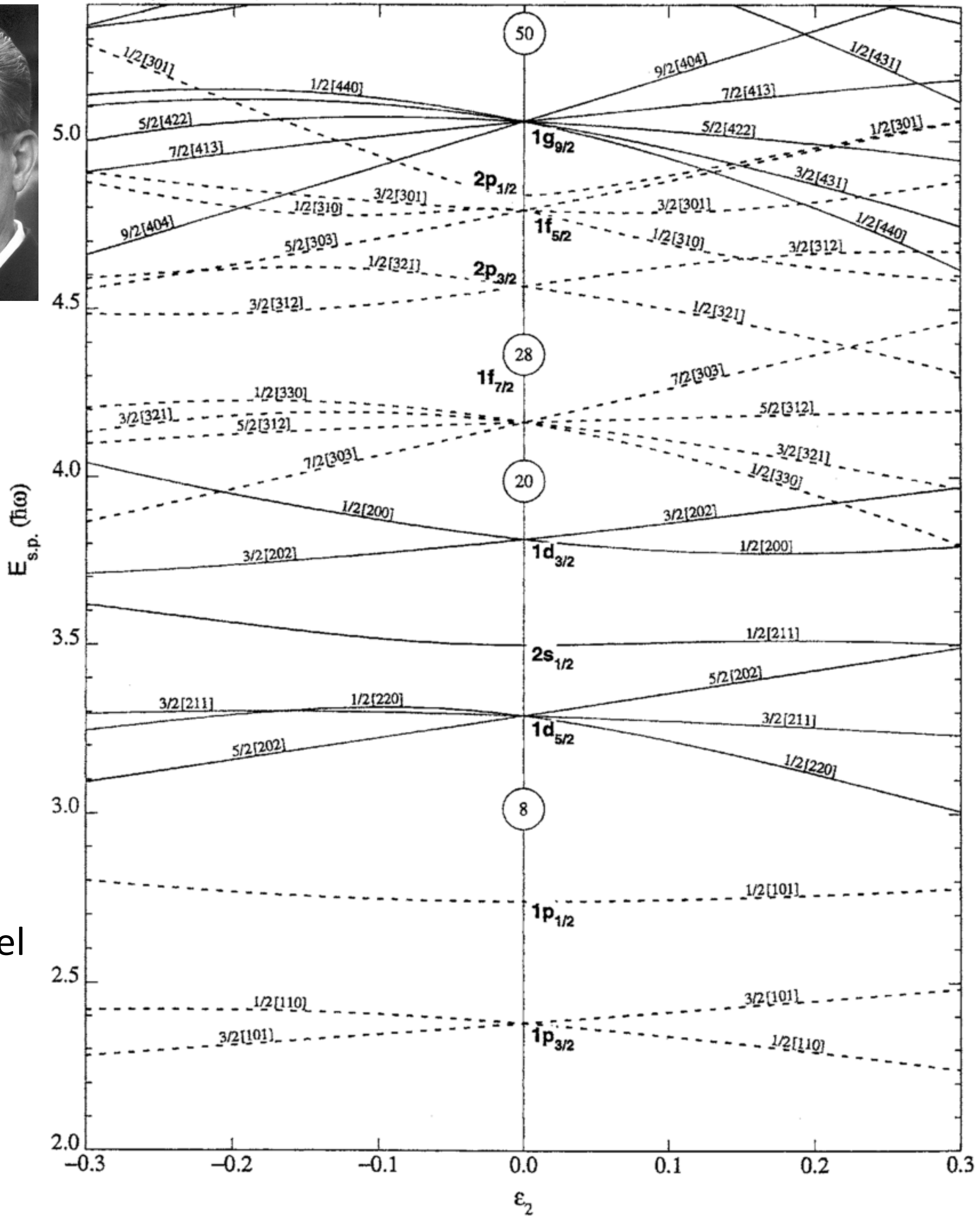

70 years later: High-resolution picture of Bohr and Mottelson's unified model

1. Take Hamiltonians from chiral effective field theory: $H = T + V_{NN} + V_{NNN}$
2. Perform Hartree-Fock or Hartree-Fock-Bogoliubov computation
   a. Yields non-trivial vacuum state $|\Phi\rangle$
   b. Informs us about nuclear deformation and superfluidity
   c. Introduces Fermi momentum $k_F \approx 1.35$ fm^{-1} as the dividing scale between IR and UV physics
   d. Allows us to normal-order H w.r.t. $|\Phi\rangle$
3. Include correlations / entanglement via your favorite method of choice (Coupled-cluster theory, Green's function method, IMSRG, …)
   a. 2-particle–2-hole (2p-2h) excitations and 3p-3h excitations (UV physics) dominate size-extensive contributions to the binding energy
   b. Symmetry restoration and collective (IR physics) yield smaller contributions that are not size extensive

Hartree-Fock computation

- Yields non-trivial vacuum (reference) state $|\Phi\rangle = \Pi_{i=1}^{A} \hat{a}_i^{+} |0\rangle$
- Reference state not unique: Can perform unitary transformations in hole space (and in particle space) without changing the physics $\hat{c}_j^{+} = \Sigma_{j=1}^{A} U_{ij} \hat{a}_j^{+}$
  - HF orbitals are delocalized (think harmonic-oscillator wave functions)
  - For input to RHIC hydrodynamics possibly want localized wave functions?

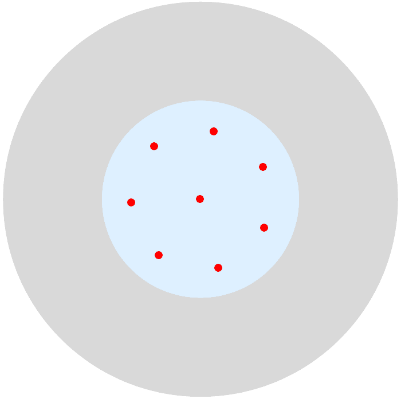

Hole space: Localized occupied HF basis functions (red points) inside nucleus (blue); distance of points $\sim k_F^{-1}$.

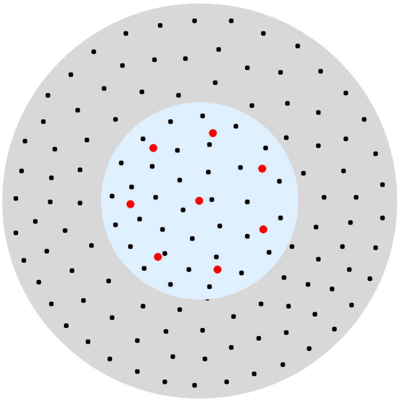

Particle space: Localized unoccupied HF basis functions (black points); distance of points $\sim \Lambda^{-1}$.

- Allows us to normal-order Hamiltonian with respect to $|\Phi\rangle$

$$\hat{H}_3 = \frac{1}{6}\sum_{ijk}\langle ijk||ijk\rangle + \frac{1}{2}\sum_{ijpq}\langle ijp||ijq\rangle\{\hat{a}_p^\dagger \hat{a}_q\} + \frac{1}{4}\sum_{ipqrs}\langle ipq||irs\rangle\{\hat{a}_p^\dagger \hat{a}_q^\dagger \hat{a}_s \hat{a}_r\} + \frac{1}{36}\sum_{pqrstu}\langle pqr||stu\rangle\{\hat{a}_p^\dagger \hat{a}_q^\dagger \hat{a}_r^\dagger \hat{a}_u \hat{a}_t \hat{a}_s\}$$

Hagen, TP et al 2007
Roth et al 2012

Coupled-cluster computations

$$\overline{H} \equiv e^{-T} H_N e^{T}$$

$$T = T_1 + T_2 + \cdots + T_A$$

$$T_1 = \sum_{ia} t_i^a a_a^\dagger a_i \ ,$$

$$T_2 = \frac{1}{4} \sum_{ijab} t_{ij}^{ab} a_a^\dagger a_b^\dagger a_j a_i$$

Correlation energy in HF basis $E_{corr} = \frac{1}{4} \sum_{ijab} t_{ij}^{ab} H_{ab}^{ij}$

- Scaling: $E_{corr} \sim A$ though $1 \le i,j \le A$
- Thus: $\sum_{ijab} \to \sum_{\langle i,j \rangle ab} \sim A$
- Only short-range correlations yield size-extensive contributions to the energy

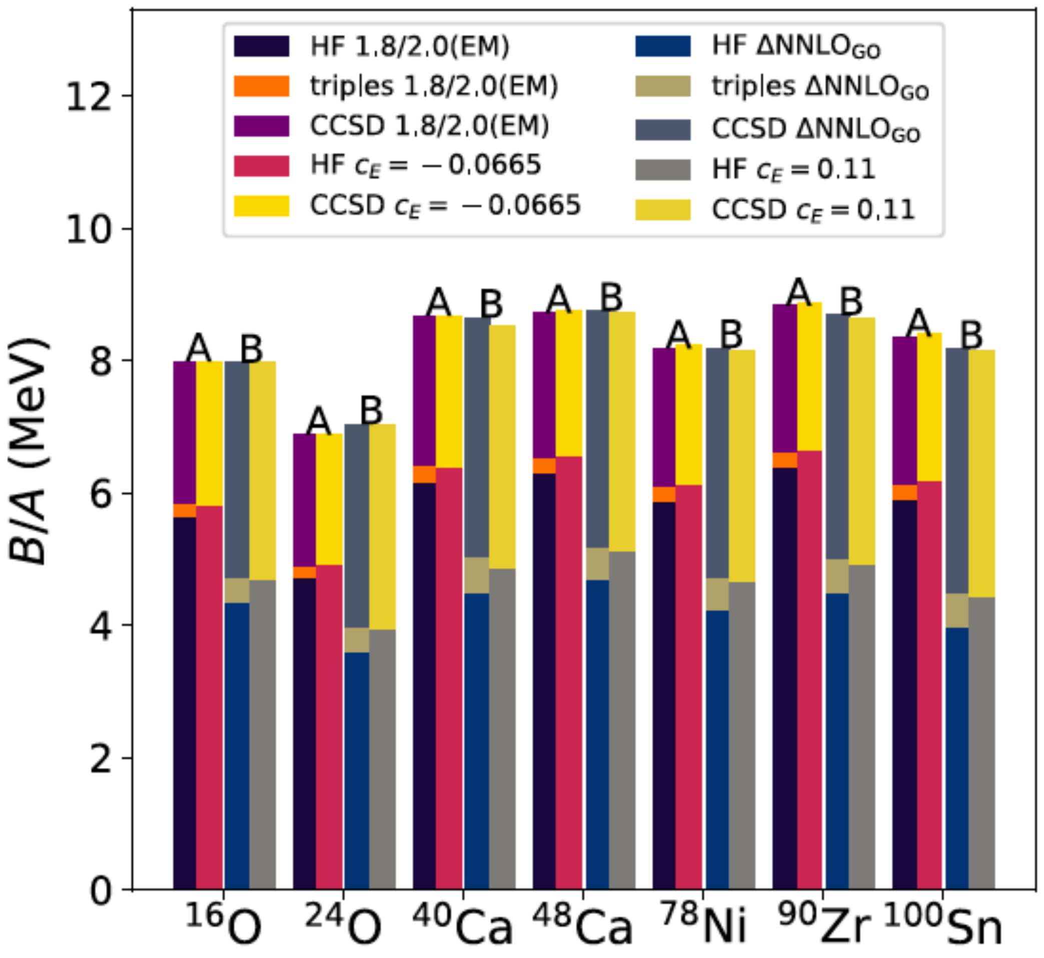

Z.H. Sun, C. Bell, G. Hagen, TP (2022)

Neutron-rich nuclei beyond $N \geq 20$ are deformed

$R_{4/2} \equiv E_{4^+}/E_{2^+}$

$R_{4/2} = 10/3$ for a rigid rotor

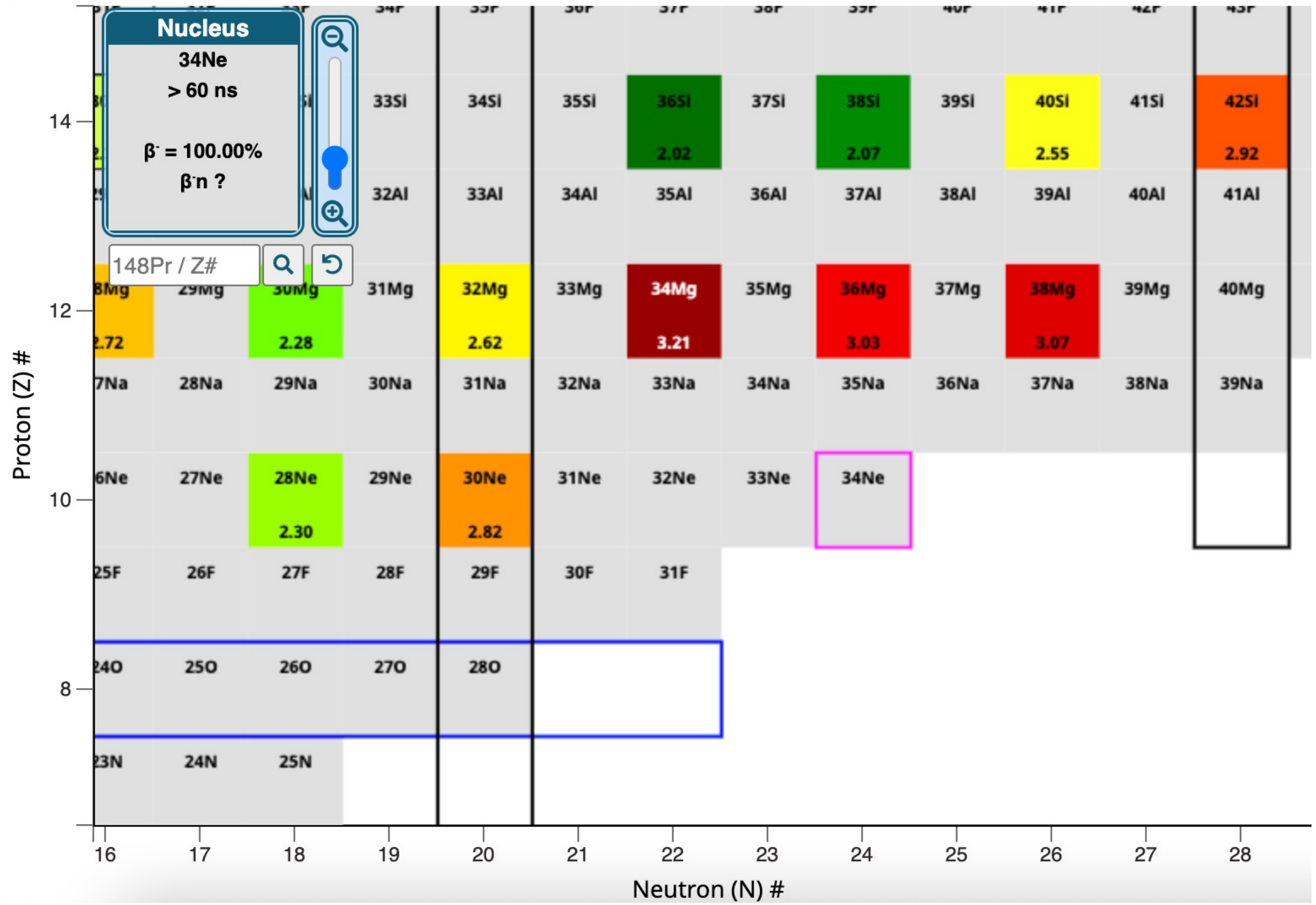

What is the structure of Ne, Mg nuclei for $N \geq 20$?

What are the spins in odd isotopes?

Where is the drip line?

"Island of inversion:" Warburton, Becker, and Brown (1990); …; Tsunoda et al 2020; …
Deformed nuclei from ab initio: Bally, Duguet, Draayer, Dytrych, Erban, Frosoni, Hergert, Launey, Ripoche, Roth, Tichai, …

Projection onto good angular momentum

Projected energies

$$E^{(J)} = \frac{\int_0^\pi \mathrm{d}\beta \sin\beta d^J_{00}(\beta)\mathcal{H}(\beta)}{\int_0^\pi \mathrm{d}\beta \sin\beta d^J_{00}(\beta)\mathcal{N}(\beta)}$$

We follow:

- Qiu, Henderson, Scuseria, …
- Tsuchimochi & Ten'no
- Duguet, …

Approach 1: Coupled cluster kernels

$$\mathcal{N}(\beta) = \langle\Phi|R(\beta)|\Phi\rangle\langle\Phi|e^V e^T|\Phi\rangle\,,$$
$$\mathcal{H}(\beta) = \langle\Phi|R(\beta)|\Phi\rangle\langle\Phi|e^V H e^T|\Phi\rangle$$

Disentangled formalism

$$e^V e^T|\Phi\rangle \equiv e^{W_0+W_1+W_2+\cdots}|\Phi\rangle$$

Approach 2: Hermitian kernels

$$\mathcal{N}_H(\beta) \equiv \langle\Psi|R(\beta)|\Psi\rangle\,,$$
$$\mathcal{H}_H(\beta) \equiv \langle\Psi|R(\beta)H|\Psi\rangle$$

$$|\Psi_{\mathrm{SQD}}\rangle \equiv e^{T_1}\left(1+T_2+\frac{1}{2}T_2^2\right)|\Phi\rangle$$

$$|\Psi_{\mathrm{SLD}}\rangle \equiv e^{T_1}\left(1+T_2\right)|\Phi\rangle$$

Benchmark computation ($NNLO_{opt}$) for ^8Be and ^{20}Ne

Benchmarks from NCSM
[Caprio, Maris, Vary & Smith (2015)]

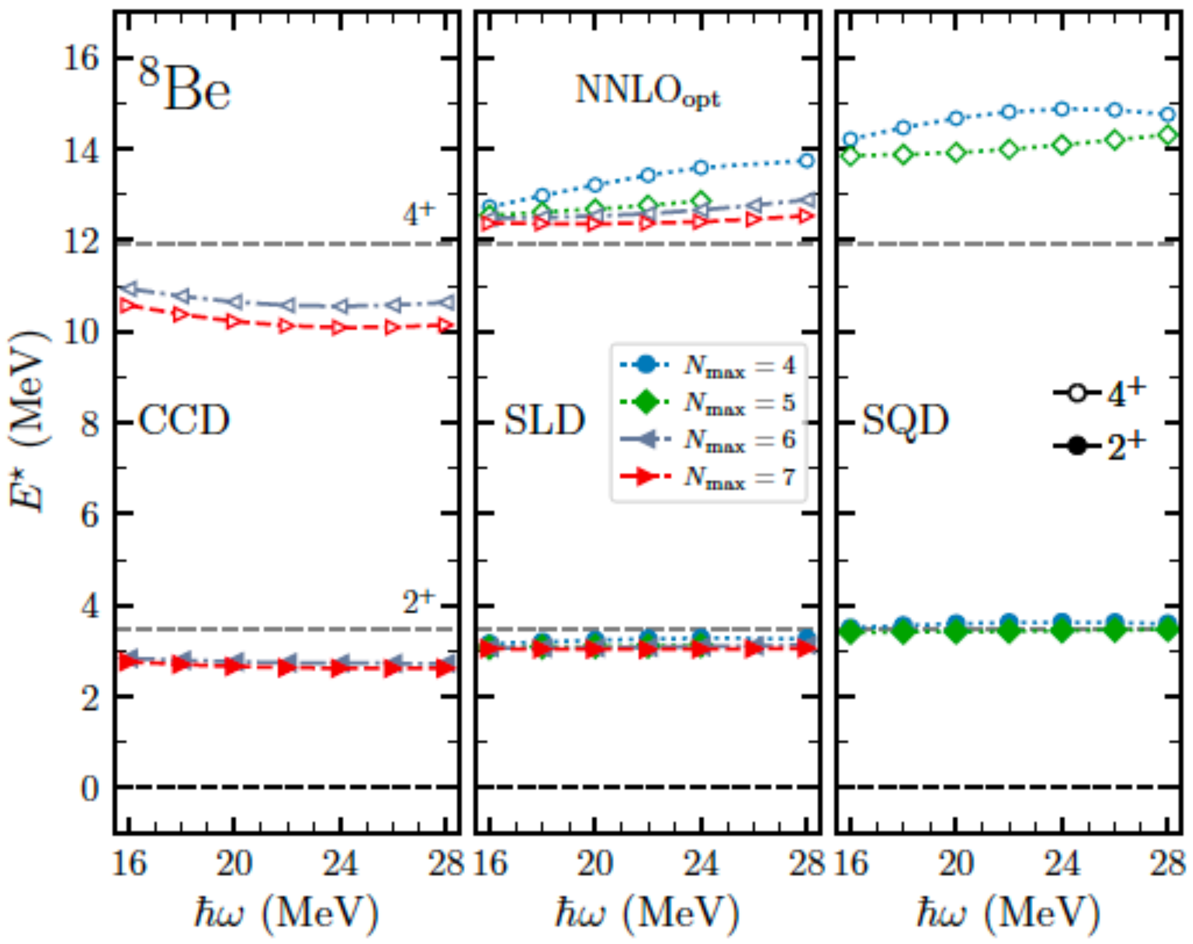

Benchmarks from Symmetry-Adapted NCSM
[Dytrych, Launey et al. (2020)]

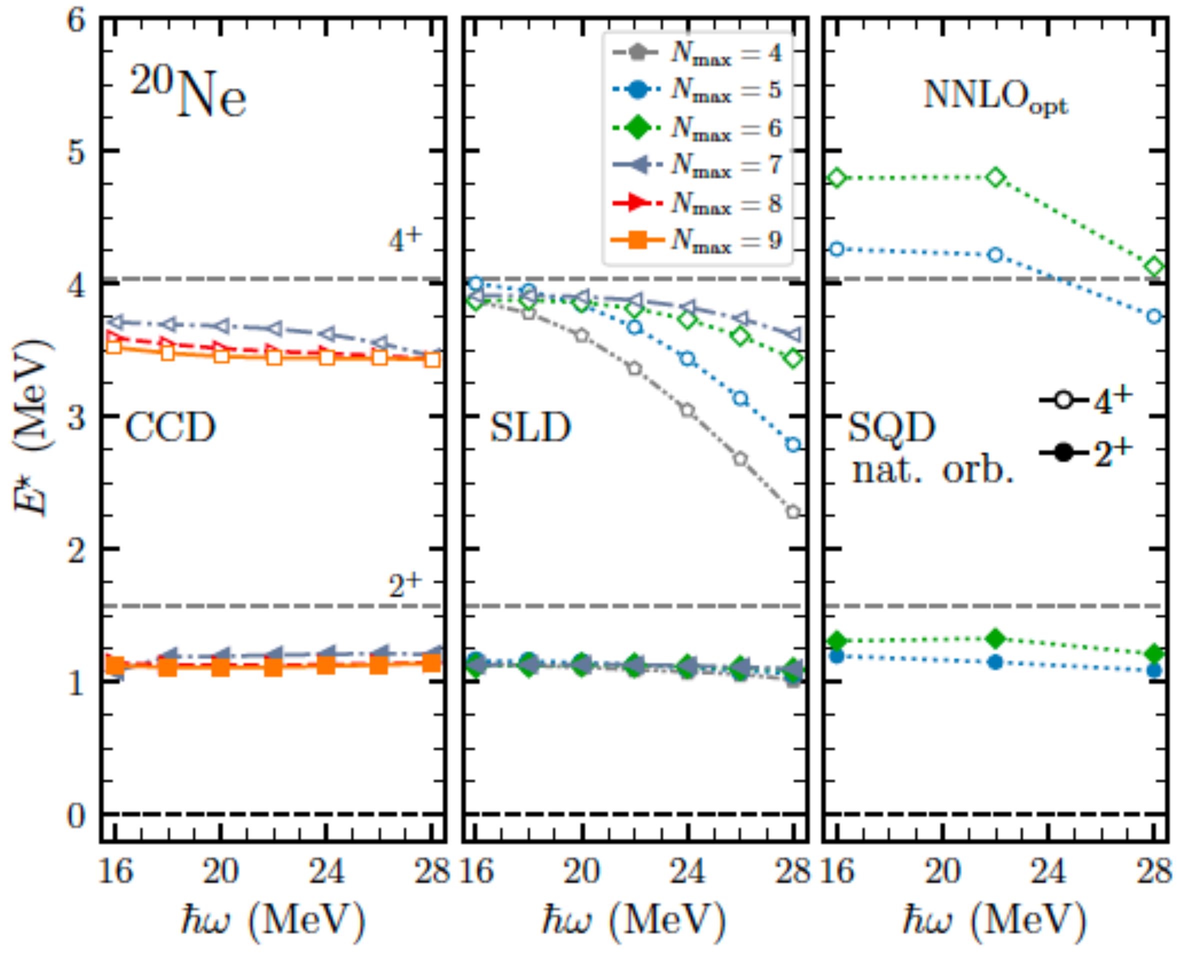

CCD spectra a bit too compressed, but we are getting there …

Hagen, Novario, Sun, TP, Jansen, Lietz, Duguet, Tichai, Phys Rev C 105, 064311 (2022)

^{34}Mg computed with NN interaction $NNLO_{opt}$

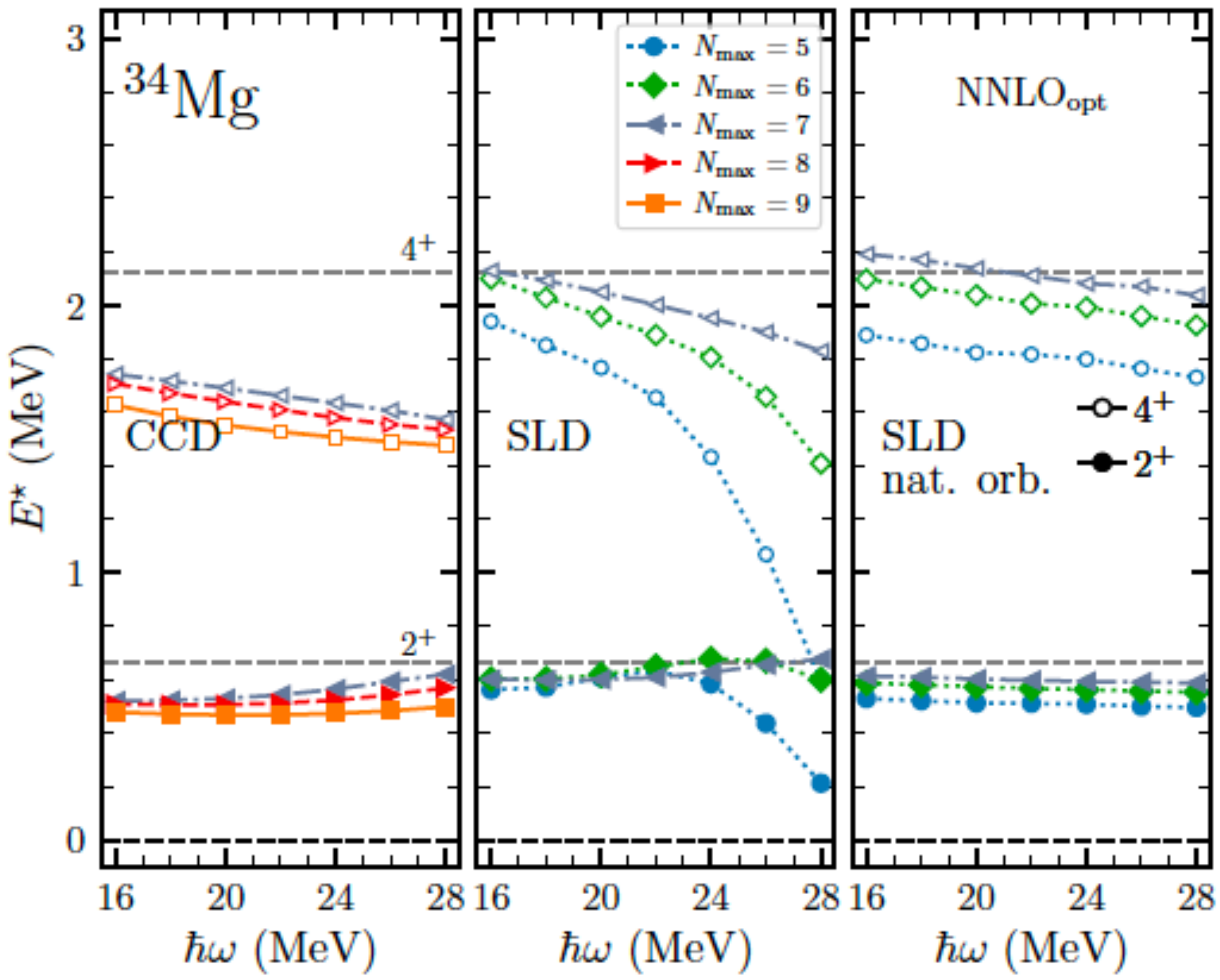

Hagen, Novario, Sun, TP, Jansen, Lietz, Duguet, Tichai, Phys Rev C 105, 064311 (2022)

^{34}Mg computed with NN interaction NNLO$_{opt}$

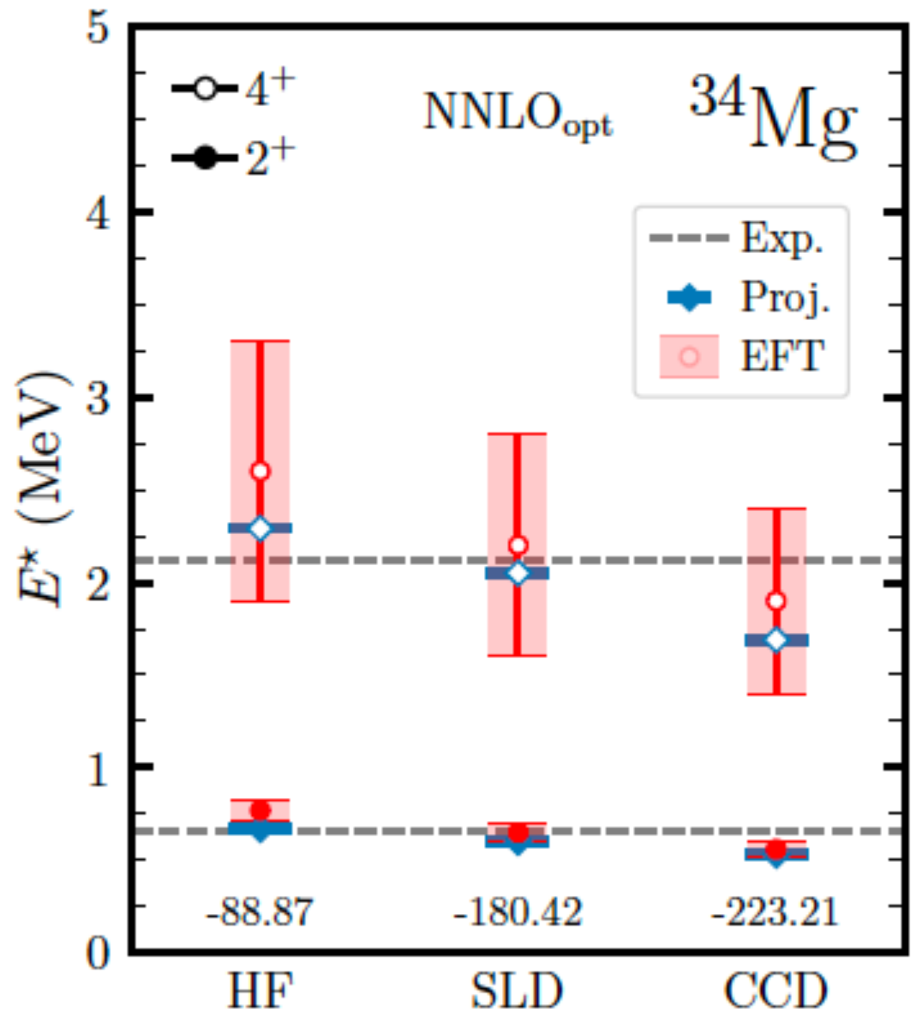

Uncertainty estimates from EFT for deformed nuclei
Input: δE from projection, $\langle J^2 \rangle$ of symmetry-broken state, and breakdown scale

EFTs for deformed nuclei [TP, Weidenmüller, Coello Pérez; Almamlah, Phillips; Chen, Kaiser, Meißner, Meng; …]

Hagen, Novario, Sun, TP, Jansen, Lietz, Duguet, Tichai, Phys Rev C 105, 064311 (2022)

Energy gain from projection decreases with increasing mass number

A rotation of the nucleus contains also *A*p-*A*h excitations.
The energy gain is not extensive (i.e. not proportional to mass number *A*)

The angular momentum expectation value decreases from Hartree-Fock (ref) to coupled cluster singles & doubles (SD) to triples (SDT-1)

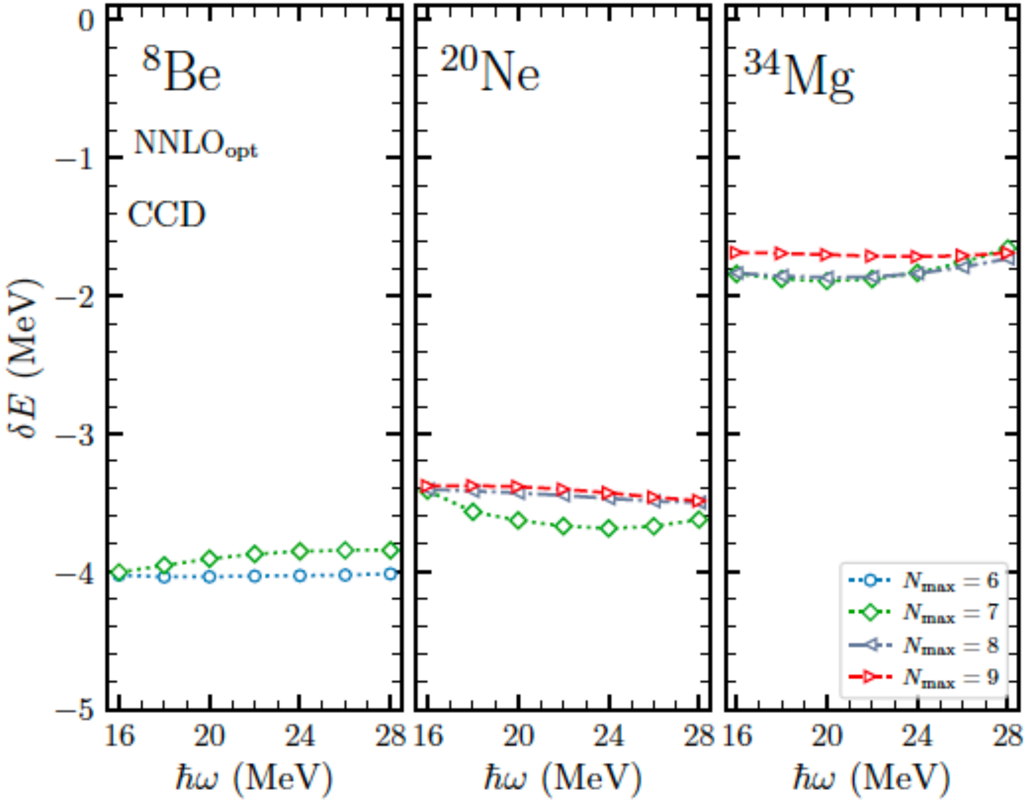

	E_{ref}	$\langle J^2\rangle_{ref}$	$\langle Q_2\rangle_{ref}$	ΔE_{SD}	$\langle J^2\rangle_{SD}$	$\langle Q_2\rangle_{SD}$	ΔE_{SDT-1}	$\langle J^2\rangle_{SDT-1}$	$\langle Q_2\rangle_{SDT-1}$	δE_{est}	E	E_{Exp}
^{8}Be	−16.74	11.17	19.46	−30.26	6.69	19.64	−3.24	5.82	18.86	−3.33	−53.58	−56.50
^{20}Ne	−59.62	21.26	35.84	−91.06	14.71	36.34	−11.27	12.09	35.71	−2.26	−164.21	−160.64
^{34}Mg	−90.21	22.62	38.56	−153.57	18.40	38.38	−20.56	15.03	36.97	−1.50	−265.84	−256.71

Intermission

- Projection of deformed coupled-cluster states onto good angular momentum works
- Good understanding of IR and UV physics involved

- Needs / wants:
  - higher precision / more controlled approximations
  - include three-nucleon forces
  - Odd nuclei

Symmetry restoration revisited

Projection after variation (PAV): $$E^{(J)} = \frac{\langle\widetilde{\Psi}|P_J H|\Psi\rangle}{\langle\widetilde{\Psi}|P_J|\Psi\rangle}$$

Right state is parametrized: $|\Psi\rangle = e^T|\Phi_0\rangle$

Left state is parametrized differently:

$\langle\widetilde{\Psi}| = \langle\Phi_0|(1+\Lambda)e^{-T}$ or $\langle\widetilde{\Psi}| = \langle\Phi_0|$ or $\langle\widetilde{\Psi}| = \langle\Psi|$

Bi-variational | Naïve | Hermitian

For axial symmetry around the z-axis the rotation operator is:

$$P_J = \frac{1}{2}\int_0^\pi d\beta \sin(\beta) d^J_{00}(\beta) R(\beta)$$

$$R(\beta) \equiv e^{i\beta J_y}$$

^{20}Ne revisited with more accurate left state

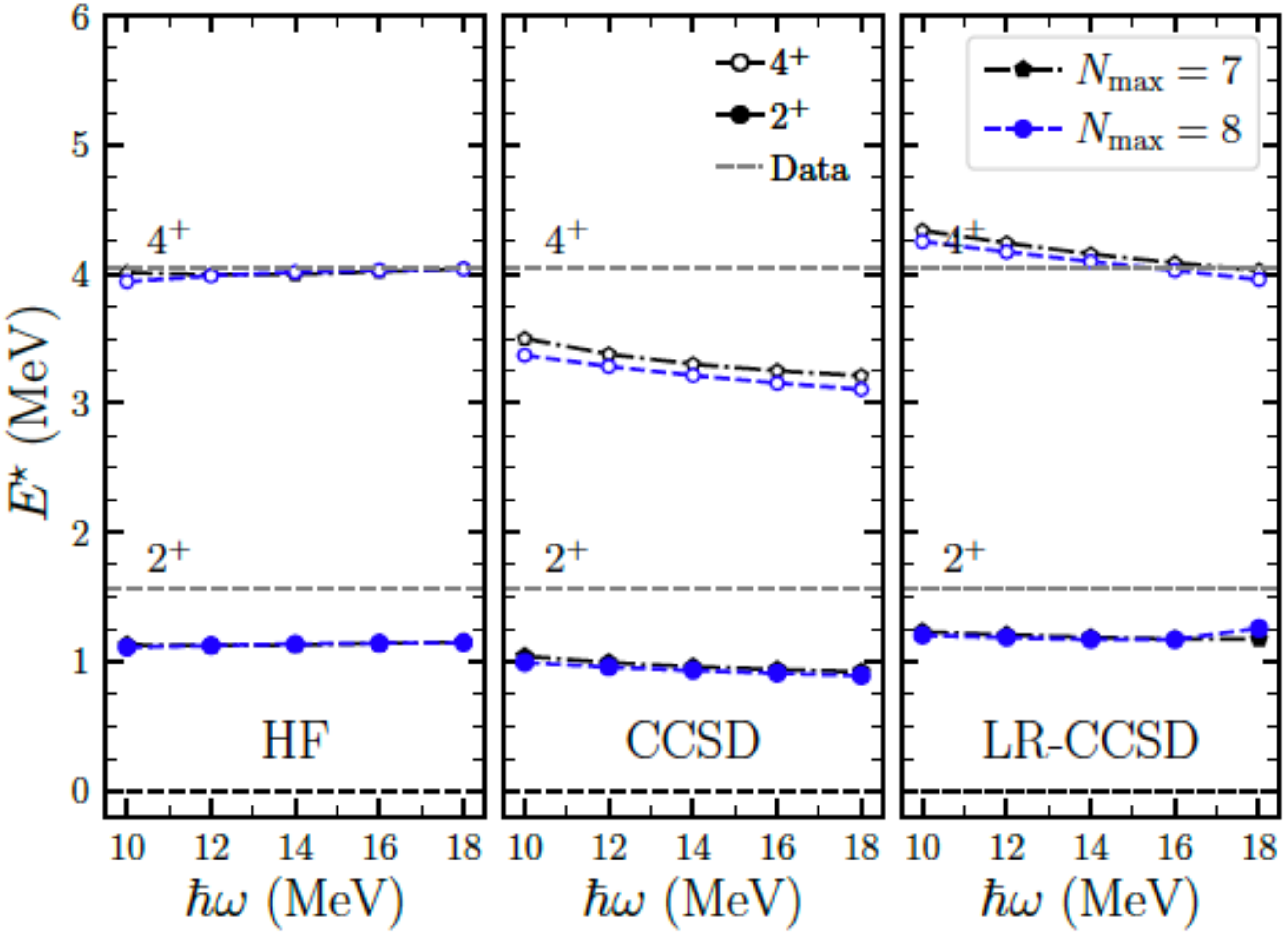

Hagen, TP et al, in preparation

Odd-mass isotopes:

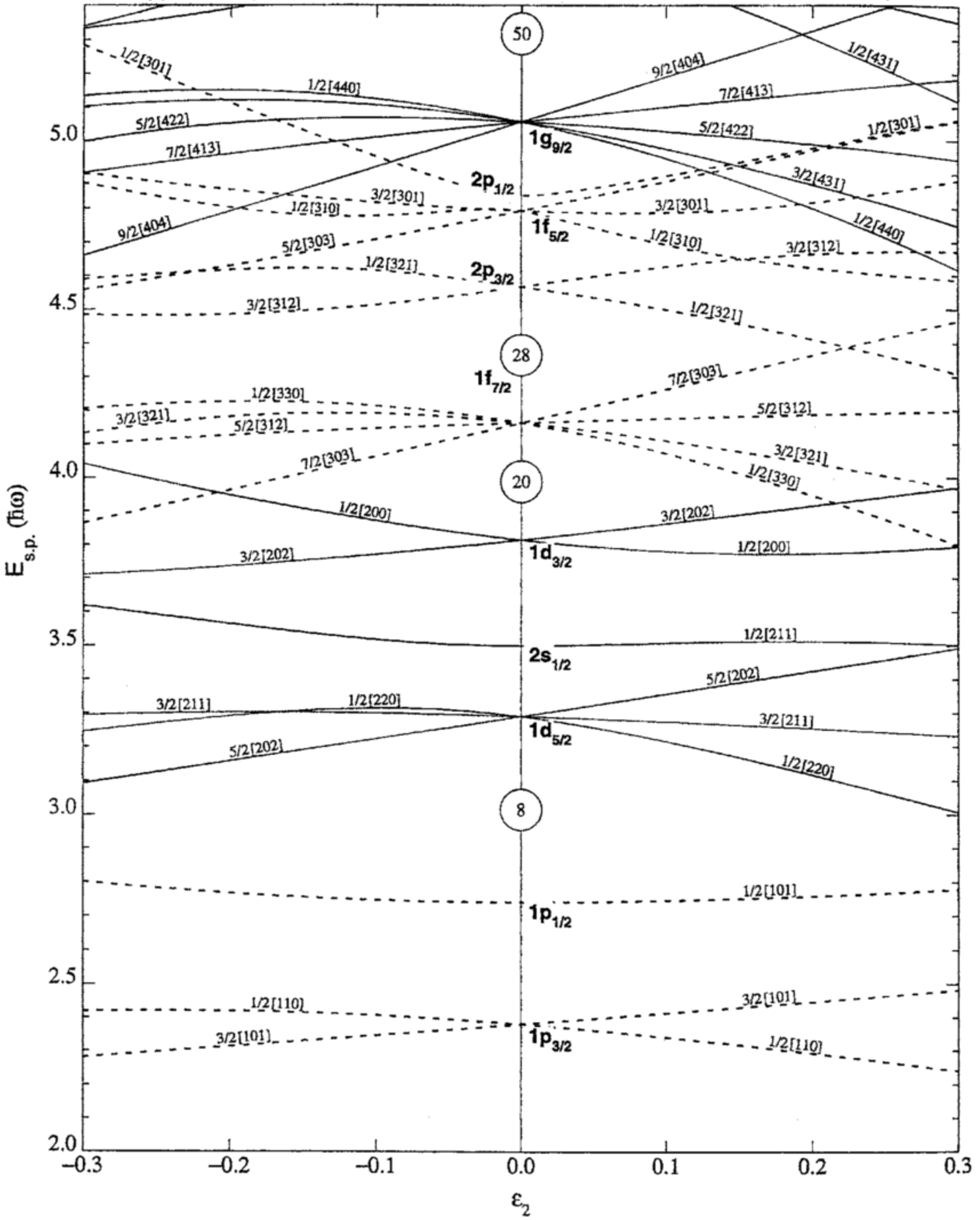

Bands computed by different filling of the odd neutron
($NNLO_{opt}$, SLD approximation)

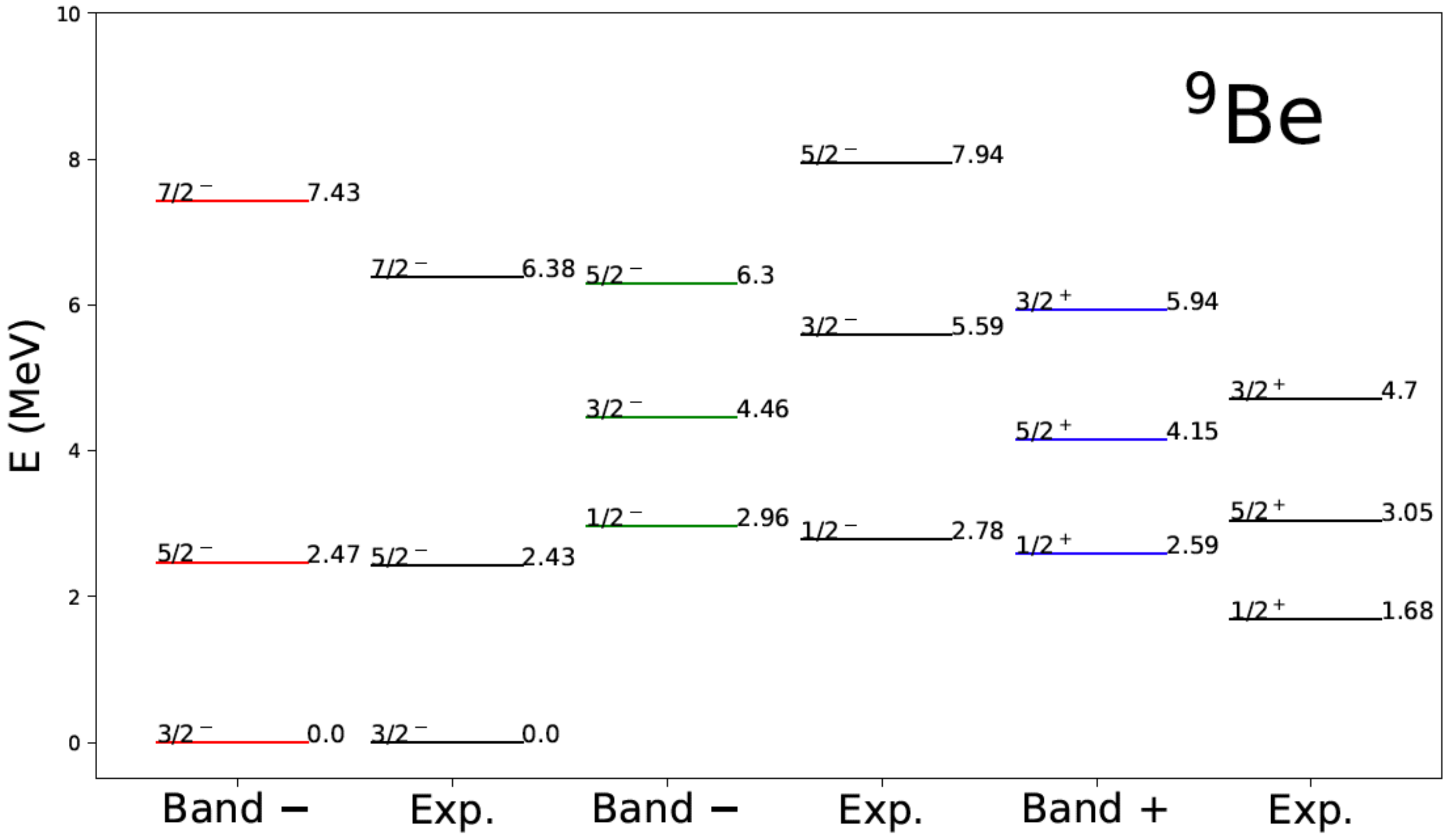

Zhonghao Sun, Hagen, TP, forthcoming

See also [Caprio, Maris, Vary & Smith (2015)]

Odd-mass isotopes

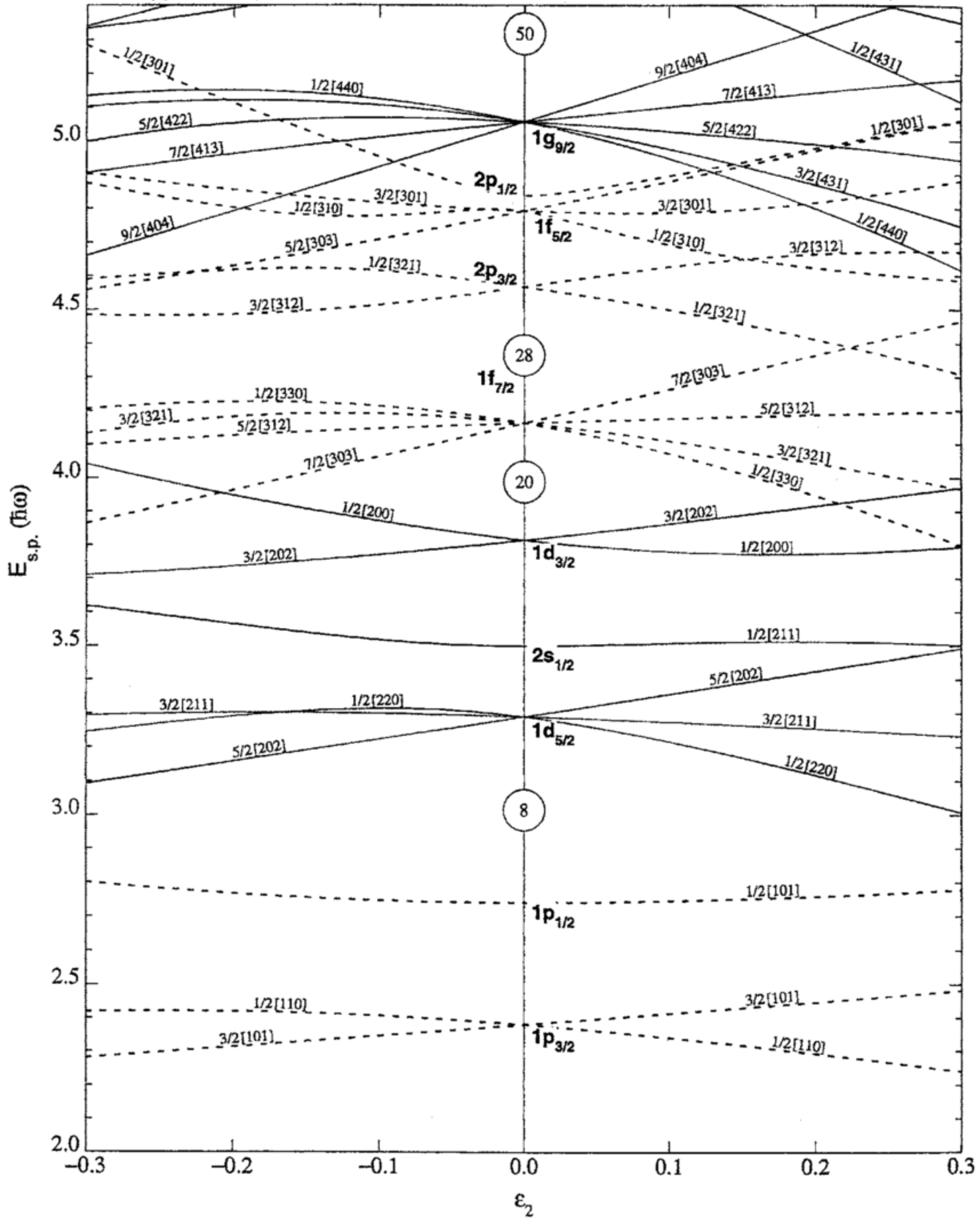

Bands computed by different filling of the odd neutron ($NNLO_{opt}$, Hartree-Fock approximation)

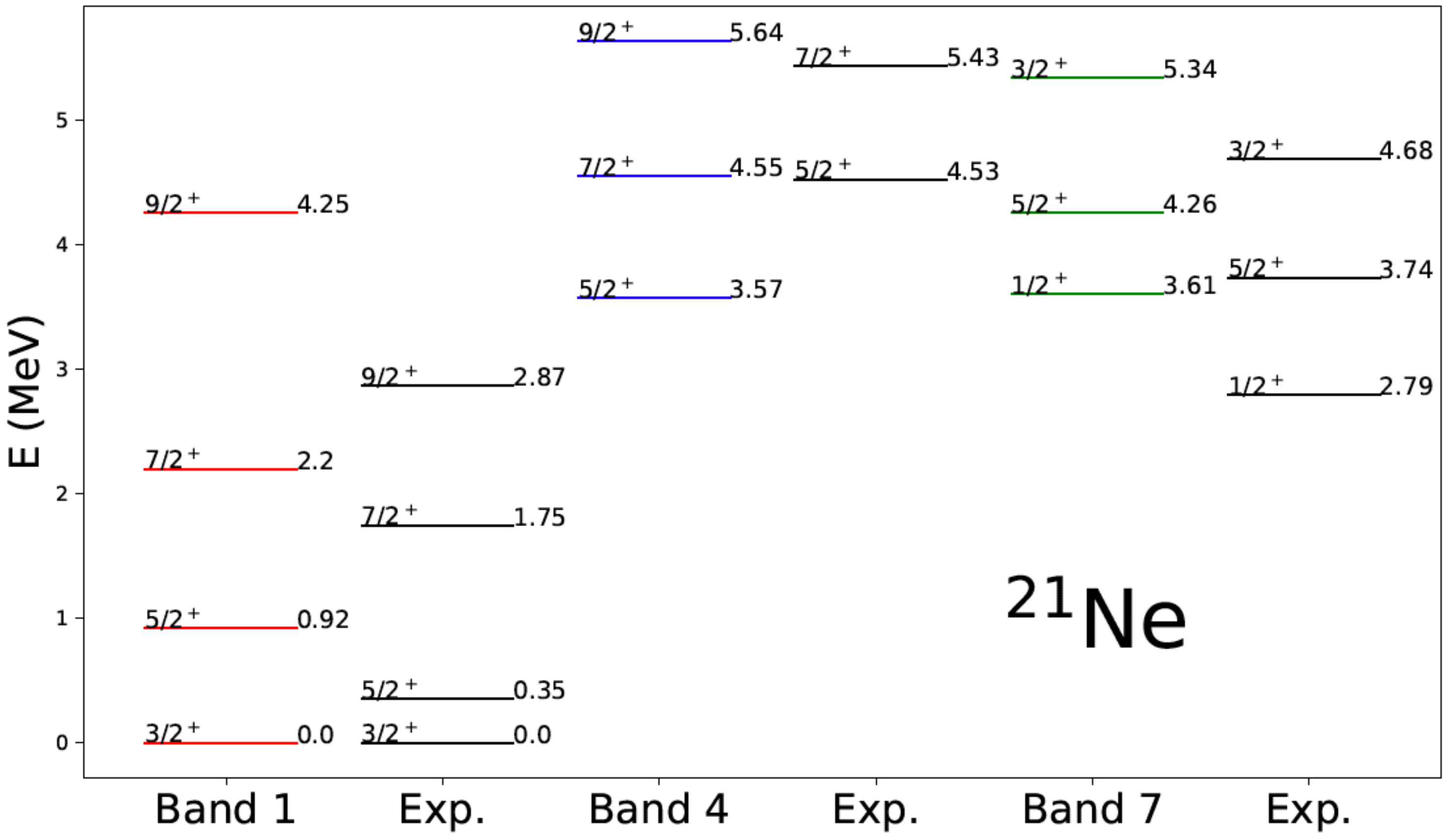

Zhonghao Sun, Hagen, TP, forthcoming

Neutron-rich neon isotopes
Inclusion of three-body forces and more accurate bra state

Perform spherical Hartree-Fock with partial filling to normal-order three-nucleon force

[→ Ripoche, Tichai, Duguet (2020)]

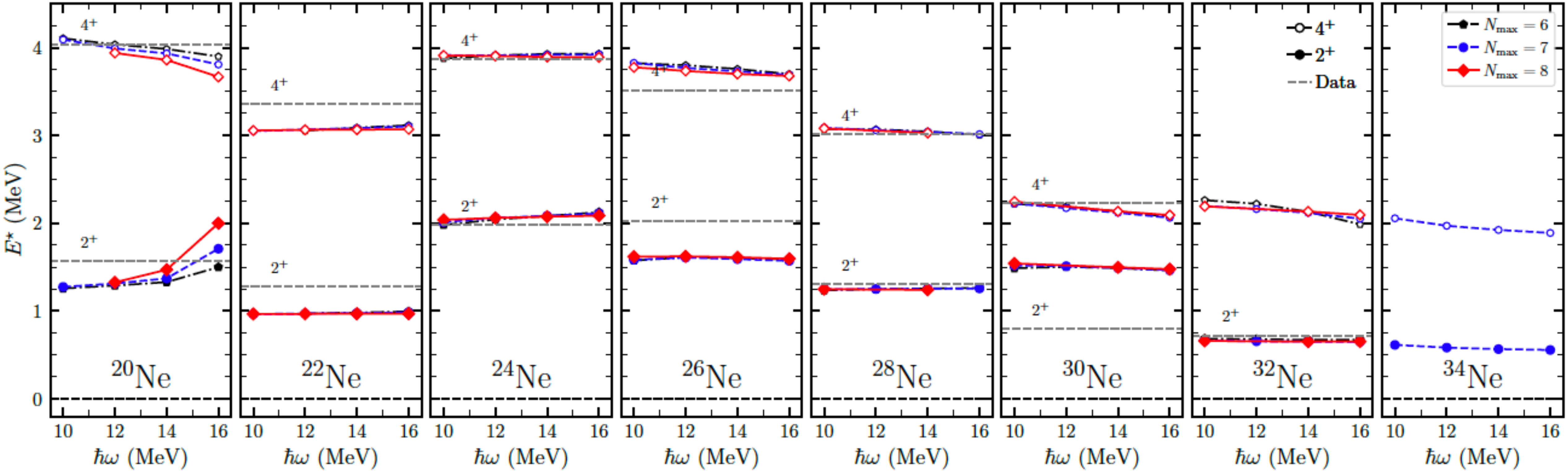

Interaction 1.8/2.0(EM) from Hebeler et al (2012); over-emphasis of $N = 20$ shell closure

^{32,34}Ne are as rotational as ^{34}Mg [Forssén, Hagen, TP et al forthcoming]

Neon isotopes with an ensemble of chiral interactions at NNLO

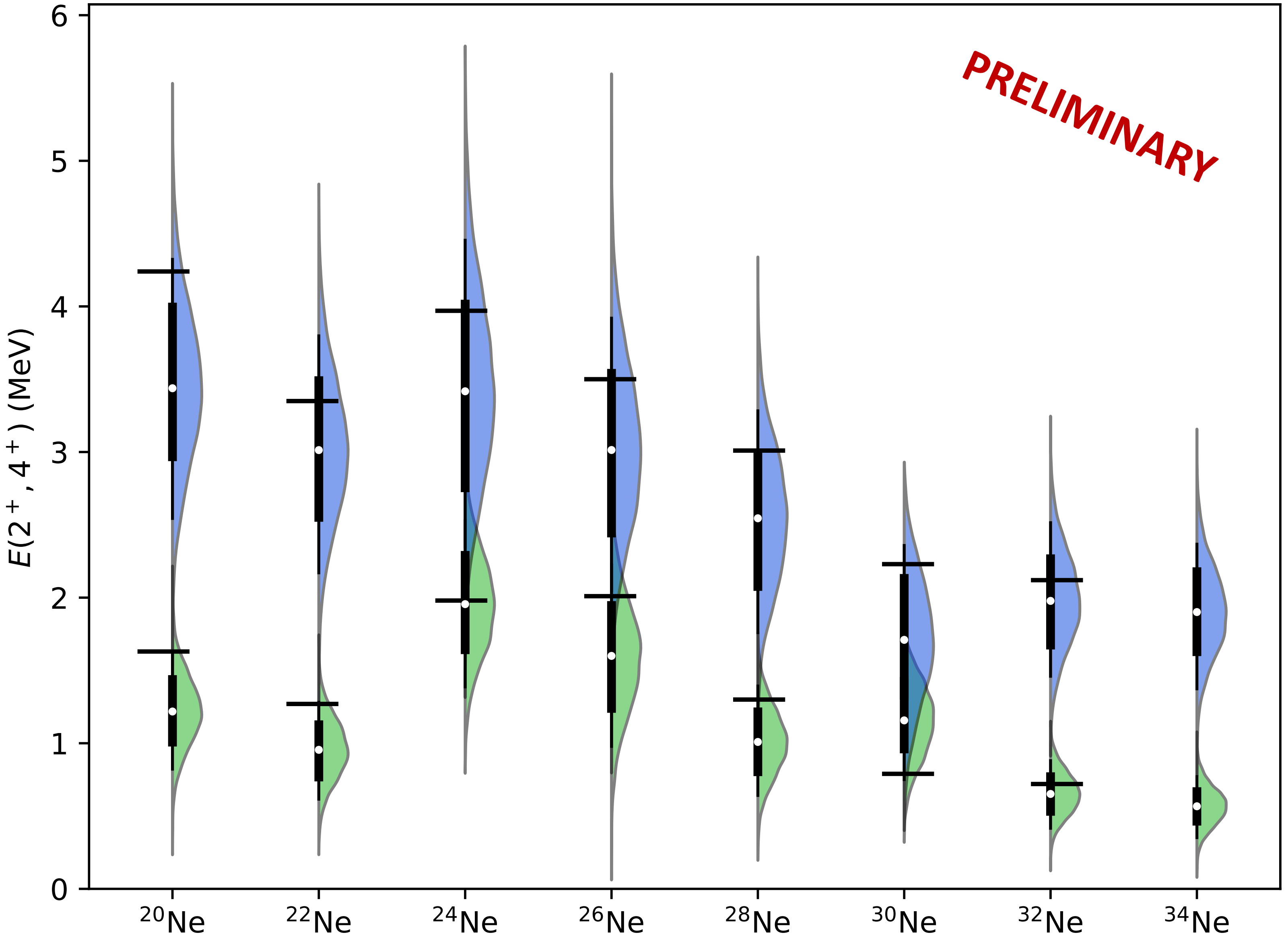

- Posterior predictive distributions for the 2^+ and 4^+ states in neon
- Spectra a bit too compressed
- Rotational structure of ^{32}Ne in good agreement with data
- We predict that ^{34}Ne is as rotational as ^{32}Ne and ^{34}Mg

[Forssén, Hagen, TP, et al forthcoming]

What causes deformation in chiral EFT?

Baranger & Kumar (1960s): Hartree-Fock computations in 1-2 shells using a pairing + quadrupole Hamiltonian

Federmann & Pittel (1979): “Deformation sets in when the T = 0 neutron-proton interaction dominates over the sphericity-favoring pairing interaction between T = 1 pairs of nucleons.”

Zuker (1997): “Multipole proposes and monopole disposes.”

What drives deformation in chiral EFT?

Results from coupled-cluster computations with angular momentum projection; based on ensemble of non-implausible Hamiltonians that predict structure of ^{28}O.

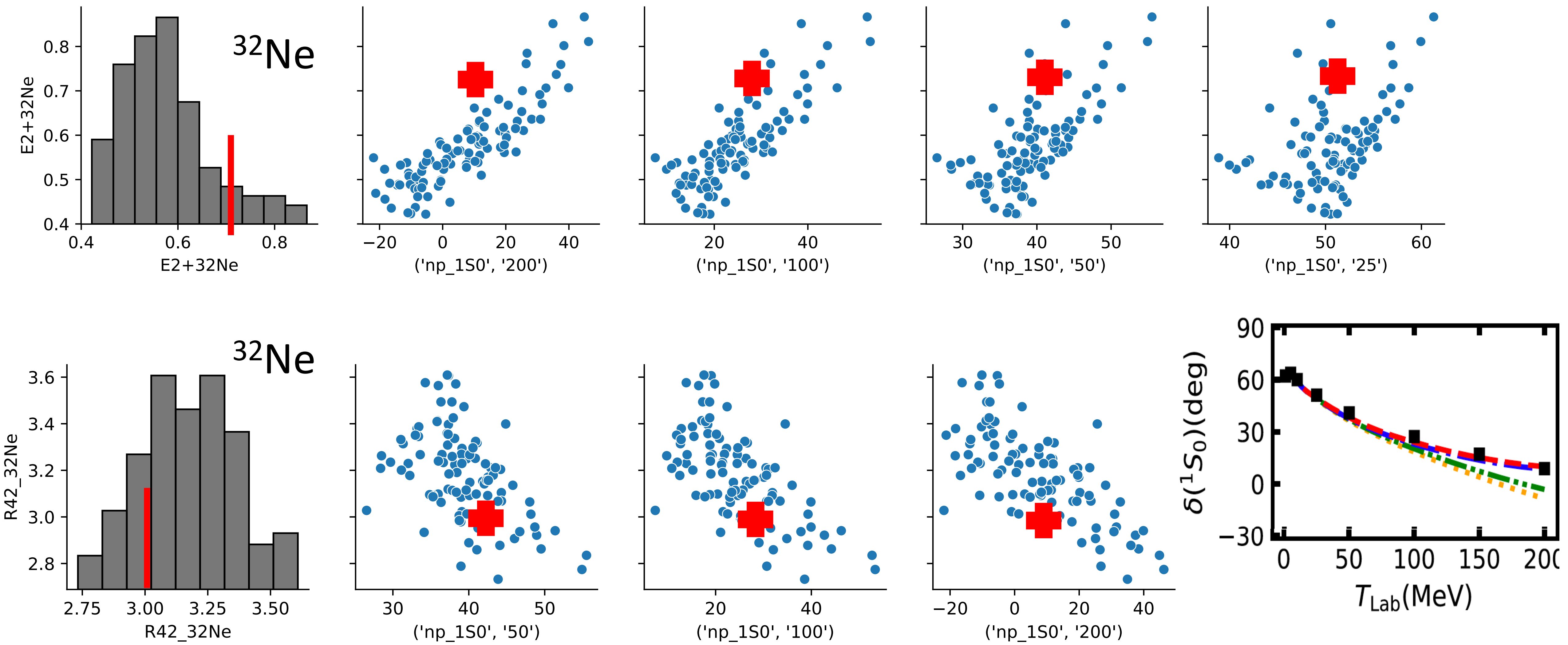

[Forssén, Hagen, TP, et al forthcoming]

What drives deformation in chiral EFT?

Results from coupled-cluster computations with angular momentum projection; based on ensemble of non-implausible Hamiltonians that predict structure of ^{28}O.

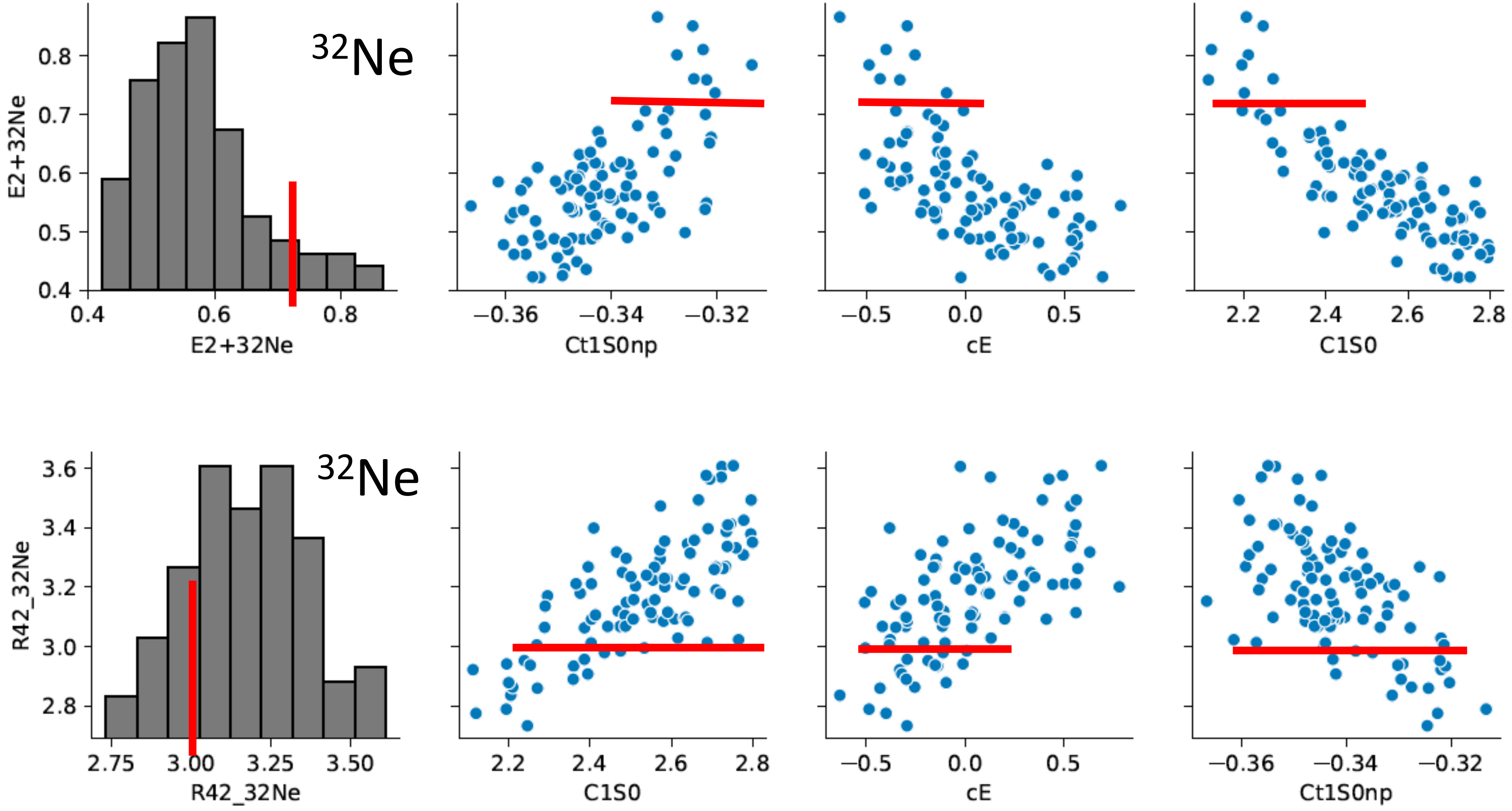

$R_{4/2} \equiv E_{4^+}/E_{2^+}$

[Forssén, Hagen, TP, et al forthcoming]

Emulation is the sincerest form of flattery...

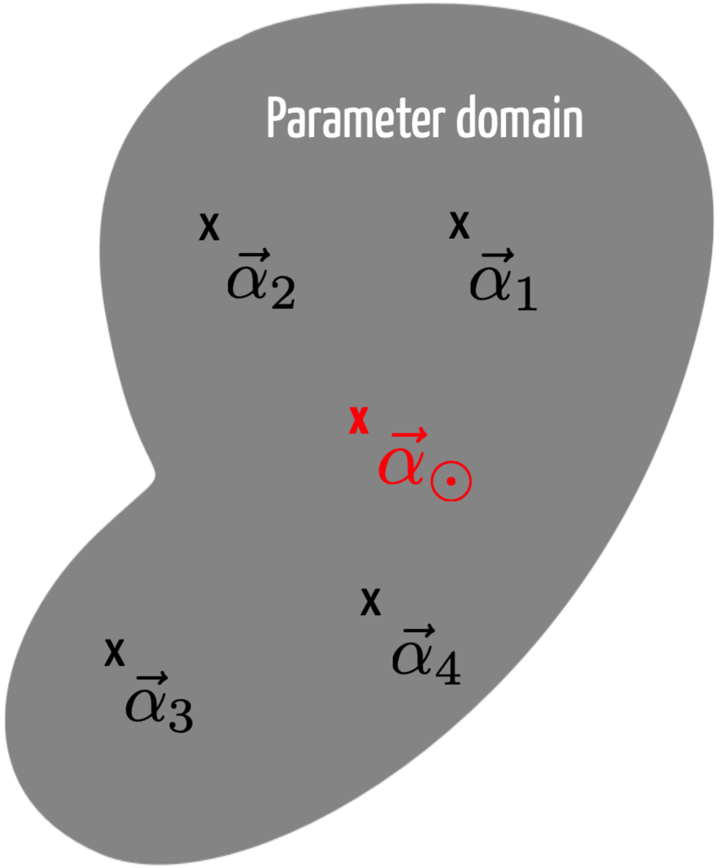

$$E^{(J)} = \frac{\langle \Phi(\alpha_{\circledcirc}) | P_J H | \Phi(\alpha_{\circledcirc}) \rangle}{\langle \Phi(\alpha_{\circledcirc}) | P_J | \Phi(\alpha_{\circledcirc}) \rangle}$$

Generalization of the eigenvector continuation method [Frame et al., (2018); Ekström & Hagen (2019); König et al (2020)]

Write the Hamiltonian in a linearized form

$$H(\vec{\alpha}) = h_0 + \sum_{i=1}^{N_{\mathrm{LECs}}=17} \alpha_i h_i$$

Select "training points" where we compute symmetry-breaking Hartree-Fock state

Project a target Hamiltonian onto sub-space of HF training vectors and diagonalize the generalized eigenvalue problem

$$\mathbf{H}(\vec{\alpha}_{\circledcirc})\, \vec{c} = E(\vec{\alpha}_{\circledcirc})\, \mathbf{N}\, \vec{c},$$

Linking deformation to microscopic nuclear forces using emulators

- Constructed accurate and efficient emulator of projected HF using 68 training vectors
- Training points obtained by using Latin Hypercube sampling within 30% of original low-energy constants

This may allow us to link deformation in atomic nuclei to underlying nuclear forces

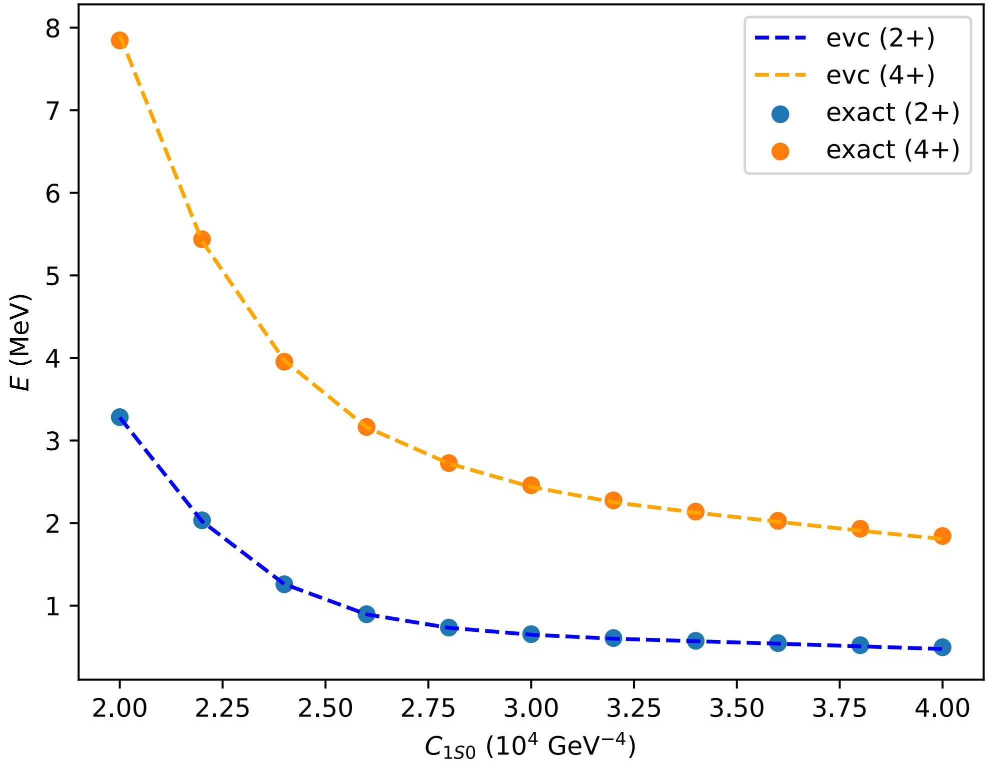

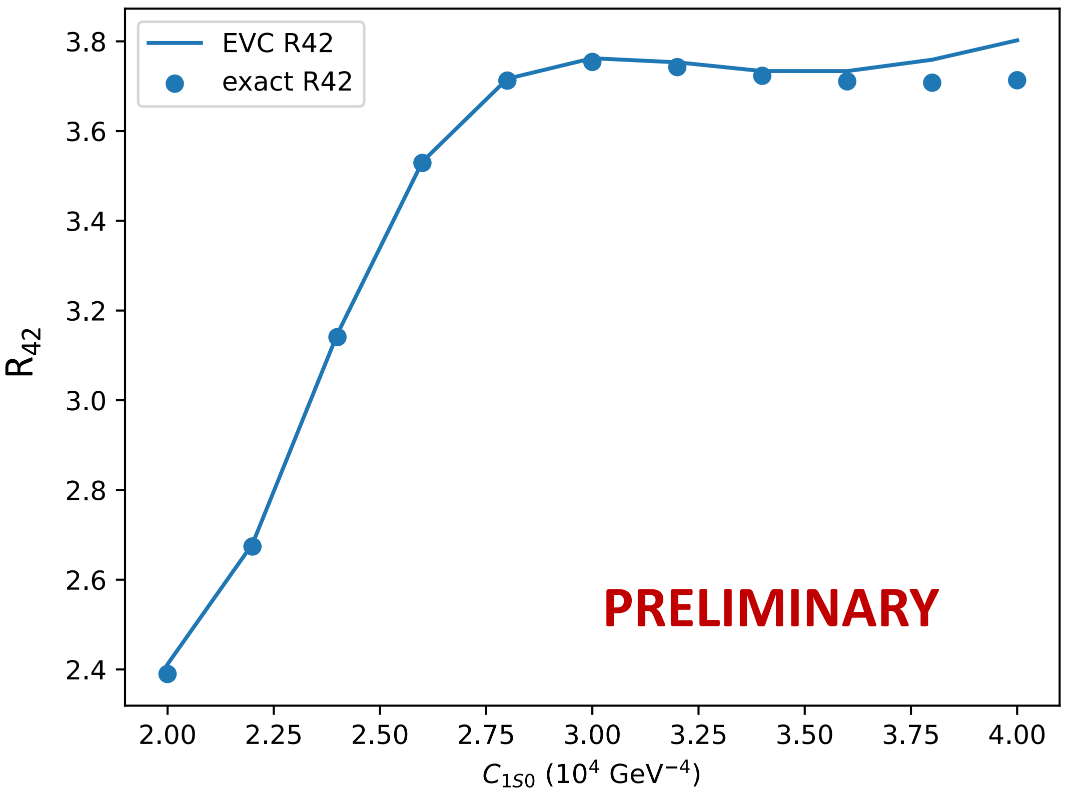

[Ekström, Hagen, TP, et al forthcoming]

What drives deformation in chiral EFT?

Global sensitivity analysis (variation of constants by ±5%)

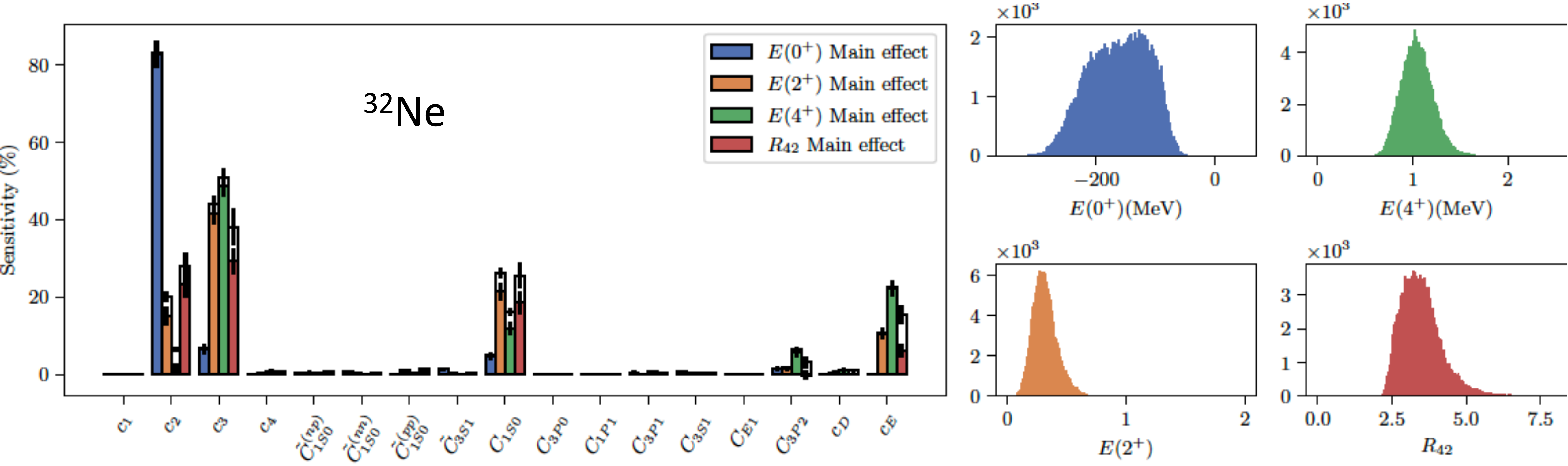

[Ekström, Hagen, TP, et al forthcoming]

What drives deformation in chiral EFT?

Global sensitivity analysis (variation of constants by ±5%)

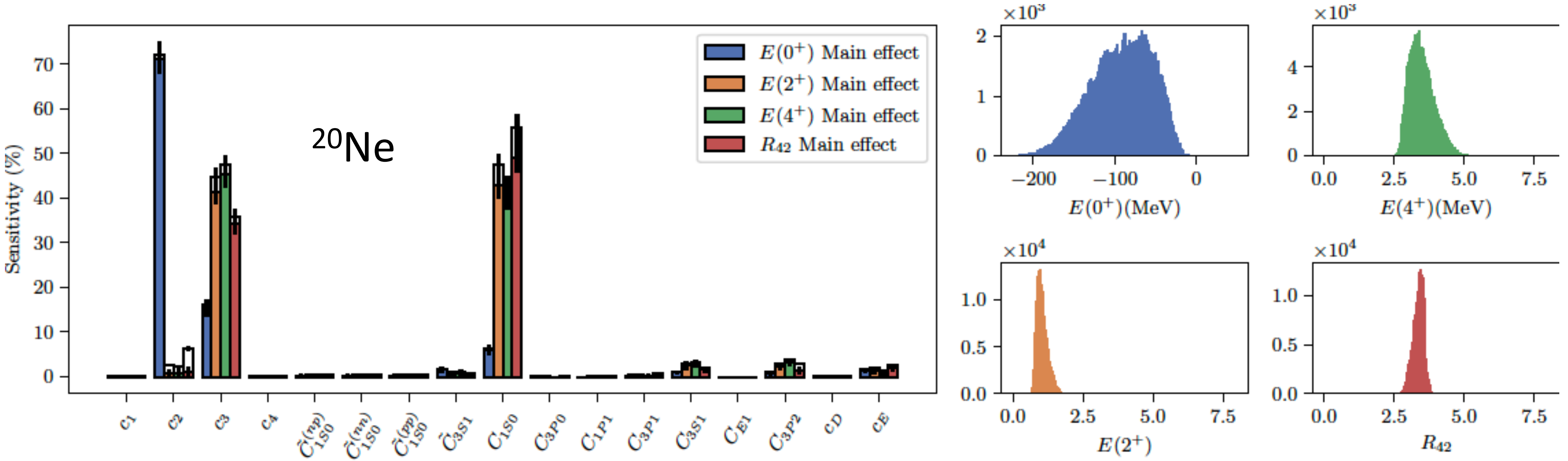

[Ekström, Hagen, TP, et al forthcoming]

Q: What drives deformation in chiral EFT?

A: In chiral EFT with Δ isobars

- $R_{4/2}$ increases with increasing repulsion of the NLO $^1S_0$ contact
- $R_{4/2}$ increases with increasing strength of the pion-nucleon coupling c_3
  - c_3 acts repulsive in NN and NNN sector $\mathcal{L} = c_3 \overline{N} \left[\dot{\pi}^2 - (\nabla\pi)^2\right] N$
- $E(2^+)$ sensitive to three-body contact in ^{32}Ne

Federmann & Pittel (1979): “Deformation sets in when the T = 0 neutron-proton interaction dominates over the sphericity-favoring pairing interaction between T = 1 pairs of nucleons.”

Zuker (1997): “Multipole proposes and monopole disposes.”

Chiral EFT, preliminary findings: the size of the repulsive forces in the pairing channel is key

Summary

- High-resolution picture of the Bohr-Mottelson unified model
  - Symmetry breaking mean-field state
  - Angular momentum projection for axially-symmetric nuclei
  - Neon isotopes: ^{32,34}Ne are as rotational as neutron-rich magnesium nuclei
  - Rotational bands in odd-mass nuclei
- First steps towards identifying what drives deformation in chiral EFT

Take home message:

1. Open-shell nuclei based on interactions from chiral EFT
2. Can provide nucleon positions, densities, …

Thank you!

Renormalizing CCSD computations

Proposal: Apply Lepage's insights to many-body computations

- CCSD lacks triples (3p-3h excitations)
- Hypothesis: Energy gain from triples are dominated by short-range correlations; renormalize via three-body contact, following Lepage (1997)

Interaction	Name	c_E
A	1.8/2.0(EM)	−0.12 [52]
A renorm.		−0.0665
B	ΔNNLO$_{GO}$(394)	−0.002 [67]
B renorm.		0.11

	Interaction and method				Exp.
	A renorm. CCSD	A Λ-CCSD(T)	B renorm. CCSD	B CCSDT-1	
^{16}O	127.8	127.8	127.5	127.5	127.62
^{24}O	166	165	169	169	168.96
^{40}Ca	346	347	341	346	342.05
^{48}Ca	420	419	419	420	416.00
^{78}Ni	642	638	636	639	641.55
^{90}Zr	798	795	777	782	783.90
^{100}Sn	842	836	816	818	825.30

Zhonghao Sun, Charles Bell, G. Hagen, TP, Phys. Rev. 106, L061302 (2022)

Renormalizing CCSD computations

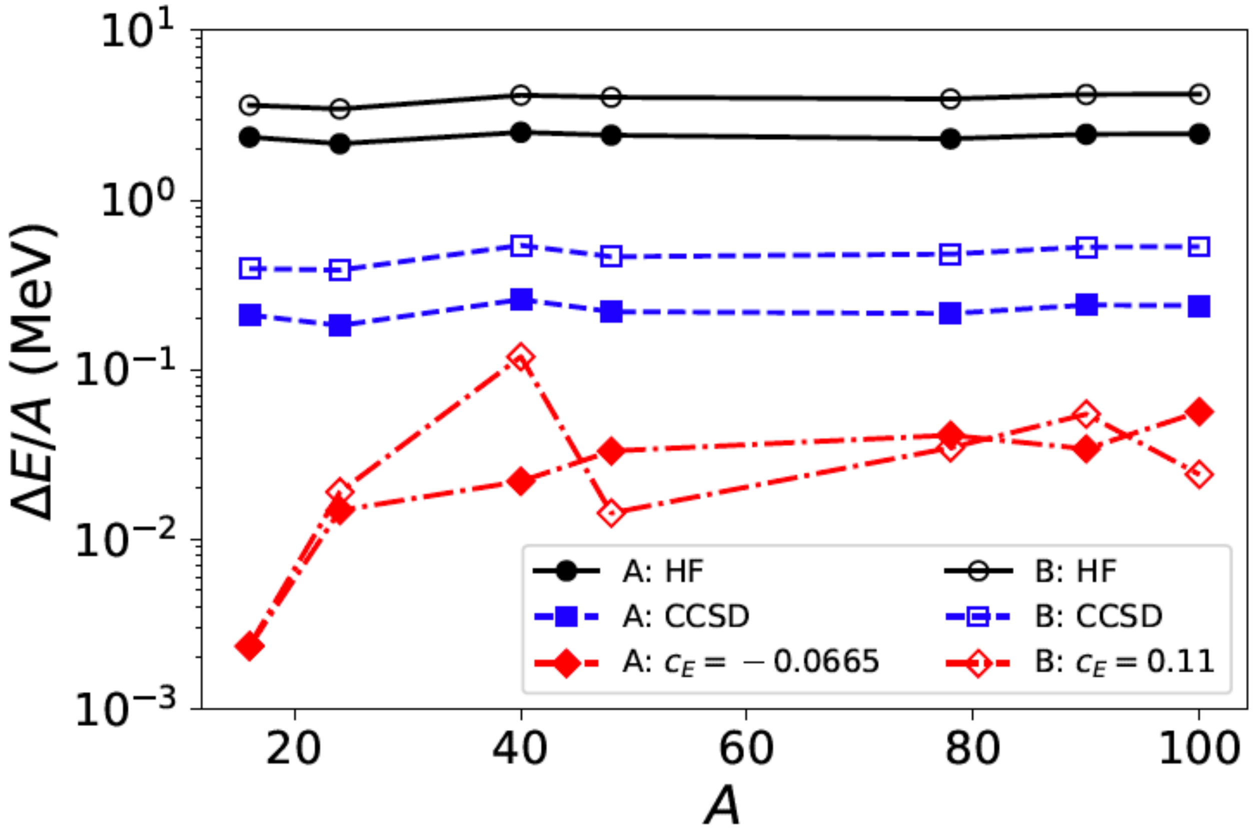

ΔE = differences to full triples

Systematic improvement from renormalization

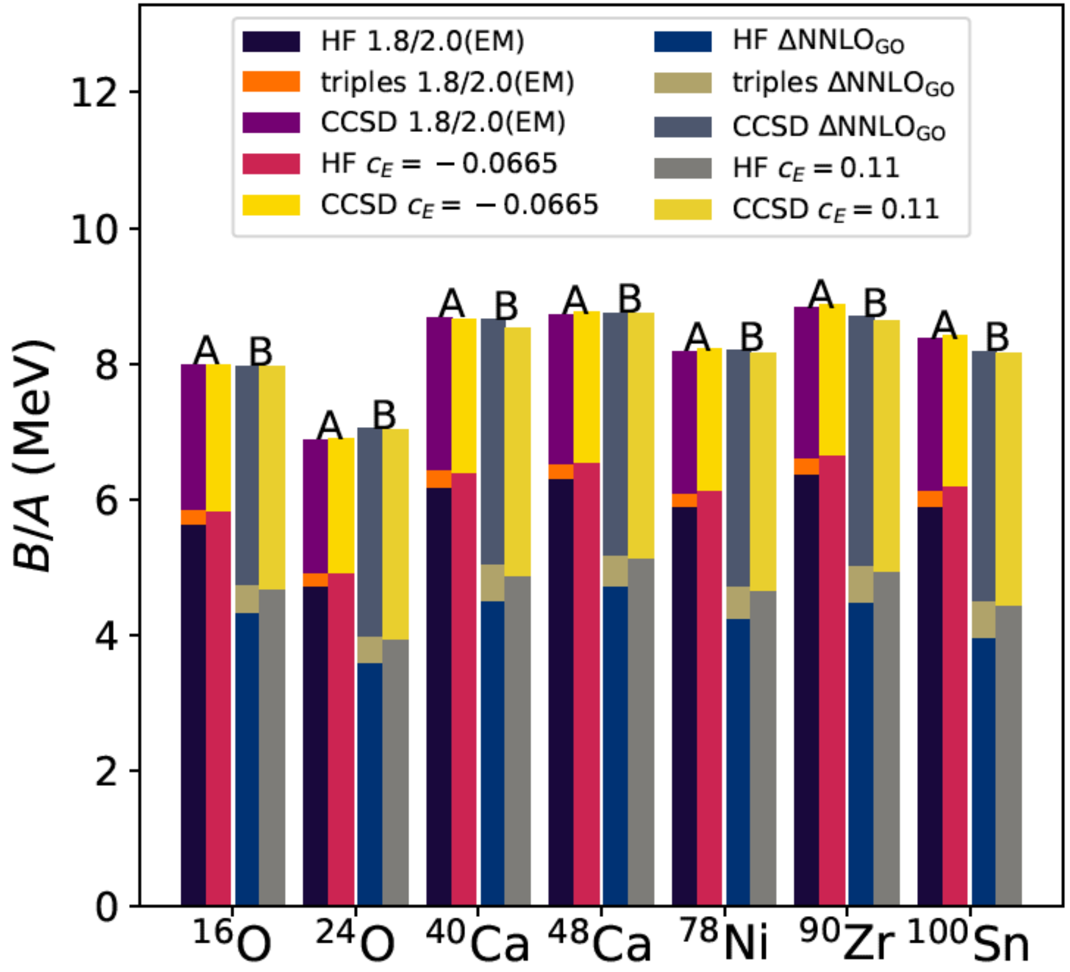

Energy from renormalization essentially goes to HF

Zhonghao Sun, Charles Bell, G. Hagen, TP, arXiv:2205.12990

Renormalizing CCSD computations

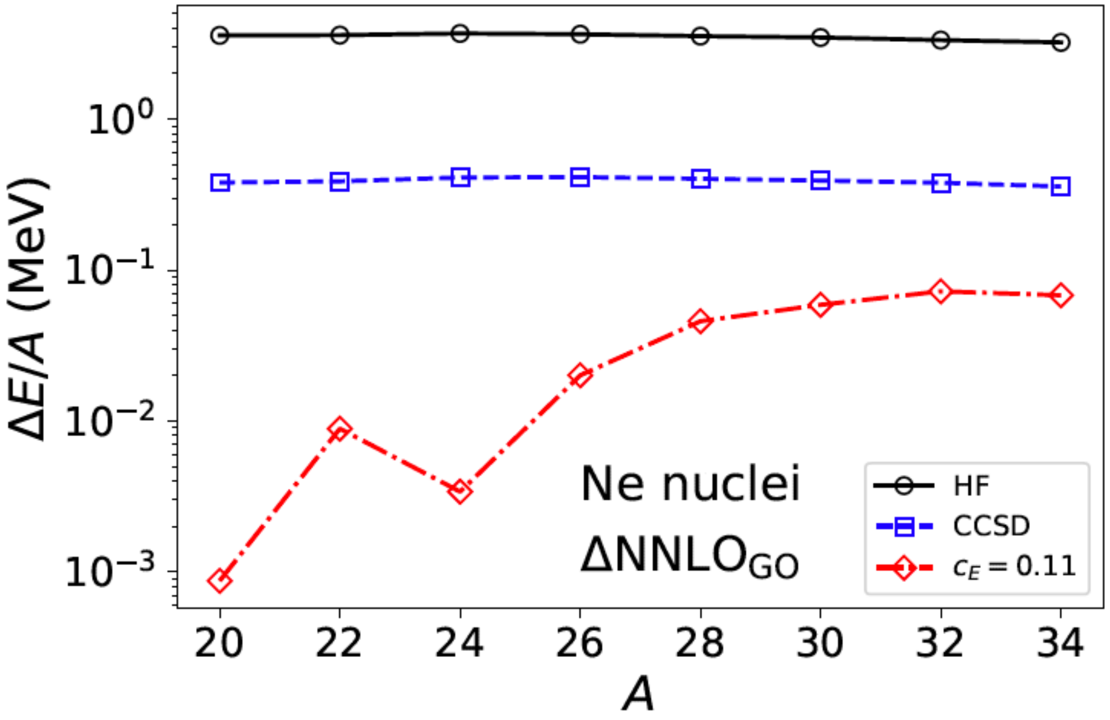

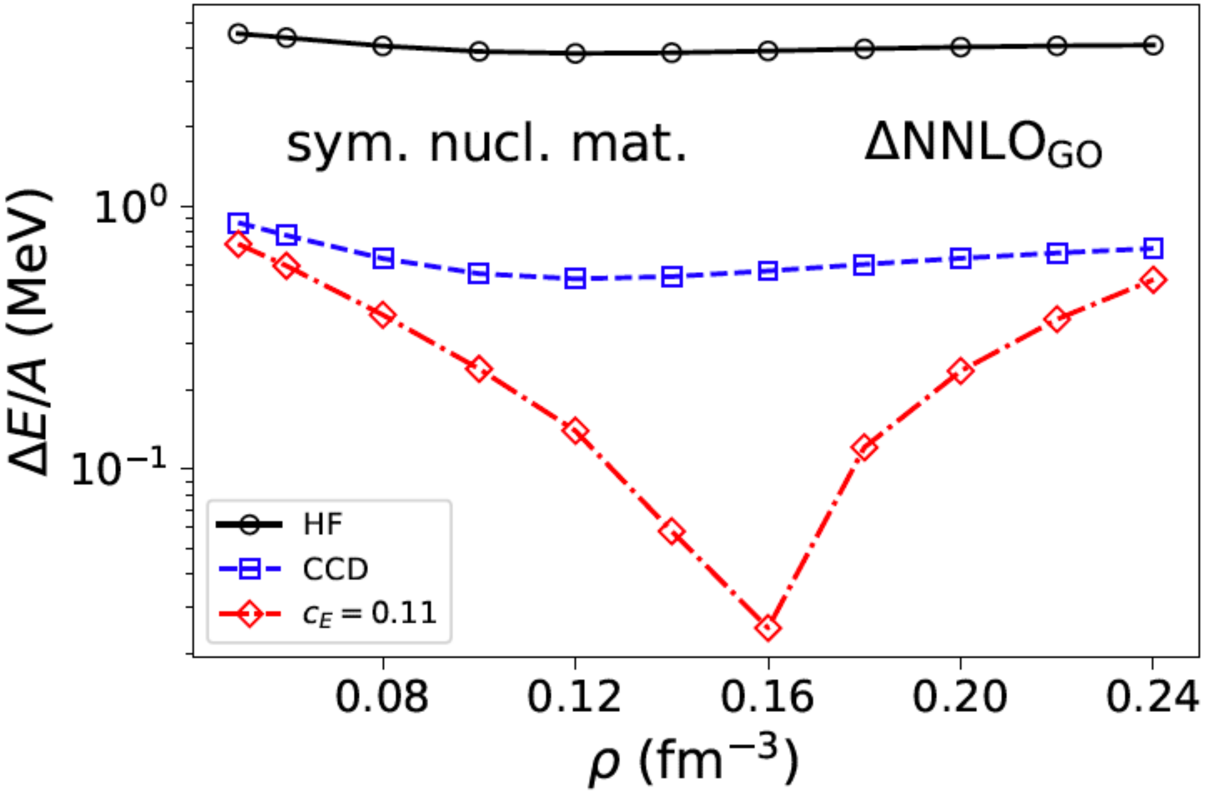

Renormalization less accurate as the dripline is approached: dilute neutron densities

Nuclear matter only accurate around saturation as $\Delta E \propto c_E\, \rho^3$in HF

Zhonghao Sun, Charles Bell, G. Hagen, TP, arXiv:2205.12990

Tower of EFTs

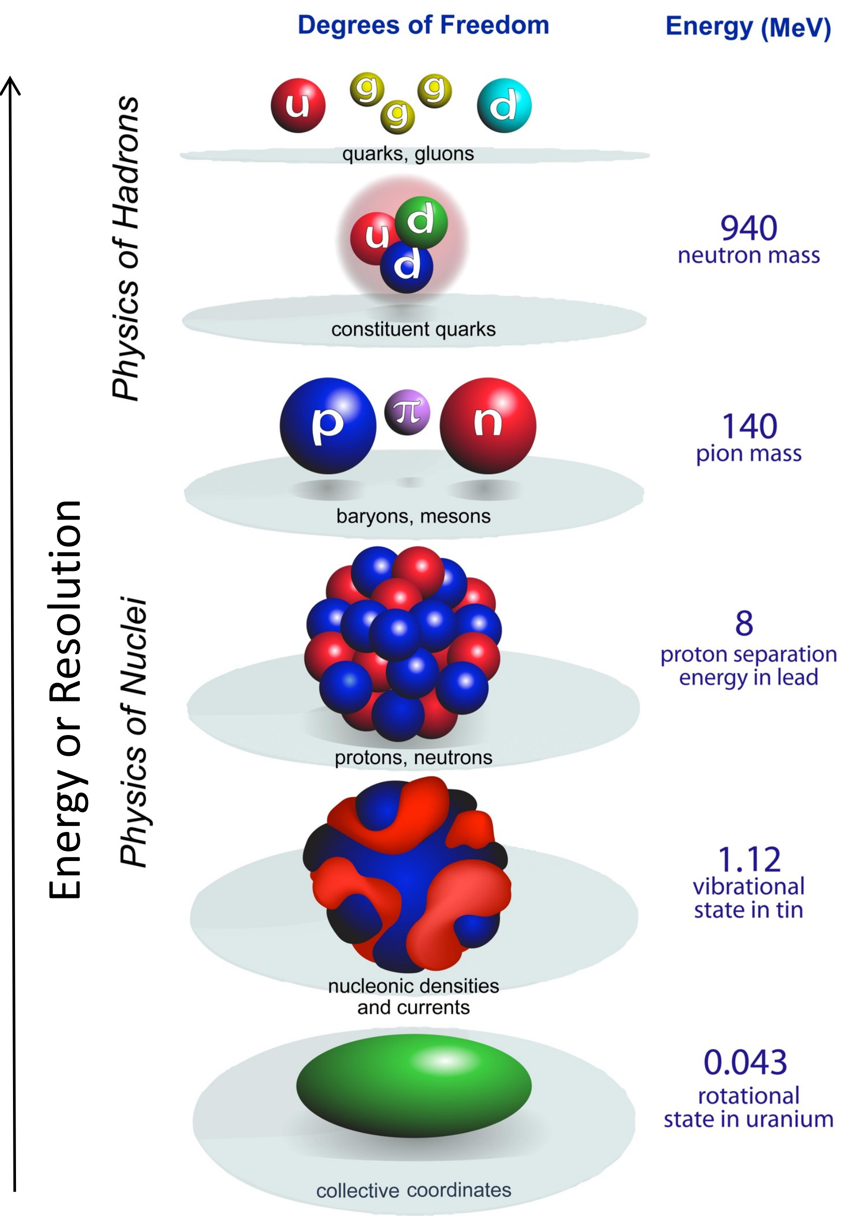

Fig.: Bertsch, Dean, Nazarewicz (2007)

EFTs can be used for uncertainty estimates on ab initio computations without symmetry restauration

Energy gain from projection of angular momentum [Peierls & Yoccoz 1957; Novario et al 2022]

$$\delta E = (E^{(0)} - E^{(2)})\frac{\langle J^2\rangle}{6}$$

Energy gain from projection of particle number [Papenbrock 2022]

$$\Delta E = \frac{1}{8a}\langle \Delta N^2\rangle$$

with pairing rotational constant from energies of nuclei with ± 1 pairs

$$a^{-1} = E_{n_0+1} - 2E_{n_0} + E_{n_0-1}$$

Note: Energy gained from projections vanish for $A \to \infty$.